

Response to Reviewers

We would like to thank the three reviewers for careful reading, insightful comments and helpful suggestions for our study. These have been included into the manuscript (see changes indicated in **bold** in the annotated manuscript attached at the end of the reviewer's response). Please find below the detailed responses (in **blue**) to the reviewers' comments and suggestions. All line indications refer to the new (annotated) version of the manuscript.

The main changes to the manuscript are listed here:

1. **Statistical Robustness of the nonlinearity and asymmetry:** A new figure has been added (figure 6), which quantifies the number of events that would have to be considered before the asymmetries and nonlinearities become statistically significant. This figure is based on a Monte Carlo approach similar to the one used by Garfinkel et al. (2018); Weinberger et al. (2019); Deser et al. (2017). This method is now also briefly described in the main text of the manuscript. Because of this, figures are re-numbered accordingly. Here we will refer to this new numbering.
2. **New supplementary material:** Following the reviewers' comments five new figures have been added to a new supplementary material. These figures include: The Rossby wave source response for the different experiments, the robustness of the SLP response as a function of the sample size (similar to Figure 5 but for each simulation), the first two EOF patterns in the North Atlantic sector in the JRA-55 reanalysis and in the model climatological simulations applying and not applying stratospheric nudging, a graphical representation of the 3 first moments of the AL and NAO PDFs shown in figure 7, and a scatter plot (similar to figure 8) showing the relationship between the NAO and AL using JRA-55 reanalysis.
3. **General text modifications:** Further details in response to the reviewers' comments have been added throughout the text. These include remarks on the effect of the stratospheric nudging, the sensitivity in SLP indices definitions and the intra-seasonal evolution of the response. This has led to a substantial increase in the length of the manuscript. We have also made an effort to shorten the text where possible.

Reviewer 1:

Recommendation: minor revisions

The authors analyze the North Atlantic sector impacts of ENSO in simulations in which nudging is applied to the stratospheric circulation to shut down a stratospheric pathway. When the stratospheric pathway is shut down, the strongest $-NAO$ response is achieved for the strong El Niño forcing, while the strongest $+NAO$ like response is for a strong La Niña forcing. However, the specific patterns are not linear, and the authors provide various diagnostics in order to explain the responses. The analysis is convincing, and nearly ready for publication.

We thank the anonymous reviewer for their constructive comments, which have been addressed in the new version of the manuscript. We answer point by point to the comments below.

Major comments:

1. The authors note that the North Atlantic response to ENSO is much weaker than that in the Pacific sector, and they don't fully quantify this effect. Recent papers by Deser et al 2017, Garfinkel et al 2018, and Weinberger et al 2019 (all cited) perform a Monte Carlo analysis to compute how many events must be subsampled from all available model simulations before a given nonlinearity becomes statistically robust, and I think a similar analysis here would be helpful. If it turns out that e.g. >50 events are needed before nonlinearities become apparent, then such a nonlinearity may not be particularly useful for seasonal forecasting purposes. However, this paper is publishable even if it turns out that nonlinearities are not large enough to be helpful.

Thank you for this constructive comment. To address this concern we have added a new Figure in the manuscript (new Figure 6), following the visualization and method used in Garfinkel et al. (2018) and Weinberger et al. (2019). This figure shows the confidence intervals of the nonlinear and asymmetric SLP response when the winters in the simulation are sub-sampled in groups of increasing size. This analysis is done for four different area weighted SLP indices, i.e. the Aleutian low, the NAO, the Azores high and the Icelandic low. The definition of these indices is introduced in the main text (lines 346-348).

The bootstrapping methodology used here is the same as described in Garfinkel et al. (2018) and Weinberger et al. (2019) and consists in randomly selecting a sub-sample of a certain size from a pair of simulations to then computing the nonlinearity or asymmetric part of the response. This calculation is repeated 2000 times for different randomly selected sub-samples in order to obtain an estimation of the associated probability density function of the magnitude that we are interesting in determining (nonlinearity and asymmetry in our case). This technique is a generalization of the bootstrapping technique we already used to assess the significance of the response in Figures 1-4, with the only difference that the entire sample size (80 winters) of each simulation is randomly shuffled to find bootstrapped distributions of the response (ENSO

forcing - climatological simulations).

By successively increasing the size of the selected sub-samples we can answer the question of how many events must be considered before nonlinearities/asymmetries become statistically detectable at a certain confidence level (in our case 95%). This is done for the asymmetry and single phase nonlinearity both for strong and moderate ENSO events and it is shown in the new Figure 6, where the box plots display the 95 and 50% confidence intervals of the asymmetry and nonlinearity of the SLP response in the different predefined regions (shown in different colors). In the plot, when the whiskers (95% confidence interval) do not cross the zero-line the nonlinearity of that specific index becomes statistically detectable using the indicated number of events. The main results of this figure are now discussed in the text (lines 320-340).

Additionally, we have now employed the same Monte Carlo technique (but using the entire sample size, as in Figures 1 to 4) to display the significant asymmetry and nonlinearity at the 95% confidence level in Figure 5, which is consistent with the results from the new Figure 6.

Minor comments:

1. Line 79: That ENSO only accounts for some 10% of vortex variability was already pointed out by Garfinkel et al 2012. The correlation of Nino3.4 with seasonal mean vortex strength is 0.3 in reanalysis and also in a range of models (see their figure 5).

We agree with the reviewer about this point and therefore we have included this point and the reference in the text (lines 83-86).

2. The studies conceptually most similar to the present one are Bell et al (2009) and Cagnazzo and Manzini (2009). While these papers are already cited, it would be helpful in the introduction to more explicitly discuss how the present analysis builds on this previous work.

We now introduce the main findings of these two papers and how the analysis in the present paper builds on these results (lines 89-94). However, while the two studies mainly focus on the importance of the stratospheric pathway, the present study focuses on the tropospheric pathway and the nonlinearity of these responses in the NAE sector.

3. Line 206 "Another interesting result is that "

Changed

4. Line 223: My understanding is that ISCA has a slab ocean at the bottom, not fixed SSTs. SSTs can be "specified" by running a tag-along Python script that computes the oceanic q-flux pattern that must be imposed in order to generate a desired SST pattern (Vallis et al 2018). If this is indeed the configuration the authors used, please clarify.

In contrast to the previous studies by Thomson and Vallis (2018a,b), in the present study as well as in Jiménez-Esteve and Domeisen (2019) we do not use a slab ocean and therefore no q-fluxes, instead we prescribe observed climatological seasonally varying SSTs as stated in line 121 of the methods section. We have now included an extra remark to emphasize this (see line 117-118).

5. Line 405: "weak an asymmetric respect to" needs to be rewritten

Thanks for pointing this out. We have now corrected this sentence.

6. Colorbar for figure 2: I find the units gdam confusing. Isn't this just dm?

gdam = 'geopotential decameters (10m)'. In our understanding, dm would be decimeters (0.1m).

We added the gdam description in the caption of that figure for clarification.

7. The North Atlantic jet seems to be too zonally oriented in the climatology (see figure 3).

This bias should be mentioned in the discussion section.

Yes, we agree with the reviewer about this model bias, which is common among many GCMs Zappa et al. (2013). We have now mentioned it in the results section as well as in the discussion (lines 499-500).

Reviewer 2 (Paloma Trascasa-Castro):

Summary:

The study addresses the tropospheric pathway of ENSO via the North Pacific to the North Atlantic using an idealised atmospheric model. They isolate the tropospheric pathway by relaxing stratospheric winds towards climatology and impose linearly increasing SST anomalies in the equatorial Pacific to simulate different magnitude El Niño and La Niña events. The study focuses on the role of quasi-stationary and transient waves for the propagation of the ENSO signal across North America and into the North Atlantic. While a nonlinear and asymmetric North Atlantic SLP response to ENSO has been previously reported in the literature, the authors found that only their strong El Niño experiment produces a response that resembles a negative phase of the NAO, whereas similar SLP responses are observed for moderate and strong La Niña events, which are of comparable magnitude to the response to moderate El Niño events. The manuscript is clear and well written and reaches substantial conclusions that add knowledge to this area of study. The analysis of the model experiments is thorough and supports the main findings.

I do have some suggestions that I believe would clarify the interpretation of the results. The relationship between the Aleutian low and the North Pacific does not appear to entirely explain the North Atlantic response simulated in the model, and therefore my suggestion is to explore other routes of the tropospheric pathway of the ENSO-North Atlantic teleconnection such as the Caribbean Sea and the tropical North Atlantic. This would also help to put the results into the context of other recent studies focusing on the Caribbean Sea.

I consider the article suitable for publication in *Weather and Climate Dynamics* after clarifying and strengthening your argument on the comments below.

Recommendation: Minor revisions

We thank Paloma Trascasa-Castro for her thorough and constructive comments on our manuscript, which have helped to improve this study. We answer point by point to her comments below.

General comments:

1. The study is explicit that it focuses on the North Pacific influence on the North Atlantic, but several studies highlight an important role for the tropospheric pathway via the tropical Atlantic (e.g., Toniazzo and Scaife, 2006; Hardiman et al., 2019; Ayarzagüena et al., 2018). Though some discussion of this broader issue is given in the Conclusions, how important is the tropical Atlantic for the interpretation of the model results shown here? A tentative hint is given on line 265, but in my view the conclusions would be strengthened if this was made more explicit. Can you explain all of the North Atlantic/European response with the mechanisms put forth in section 6? If the model does not simulate a pathway via the Caribbean Sea is this a limitation of the model? Or are there limitations of other studies that have argued for an important role for the tropical Atlantic pathway, e.g. they have neglected the North Pacific downstream effects?

We agree with the reviewer that the total North Atlantic response cannot be explained alone due to the downstream propagation of transient and quasi-stationary (QS) waves from the North Pacific as outlined in section 6 of the paper. However, the model response of the horizontal wave fluxes across North America explain reasonably well most of the nonlinearities observed in the North Atlantic response as shown in the old Figure 9 (new Figure 10). In the manuscript, we recognize that other pathways can contribute (see for example lines 54-56). In the present study we decided to focus on the North Pacific role, while leaving the contribution of the Caribbean and Tropical North Atlantic pathway for future work, while acknowledging its likely contribution.

Nonetheless, to answer the previous question, we have assessed if the model is able to simulate a pathway through the Caribbean Sea – Tropical Atlantic via a remote anomalous Rossby wave source in this region. We find that this can indeed be considered a relevant mechanism but mainly for the strong El Niño forcing (see the new supplementary Figure S1). Other studies (e.g., Ayarzagüena et al., 2018; Toniazzo and Scaife, 2006) have shown that the Tropical Atlantic pathway might be more relevant during early winter (ND) than late winter (JFM), when the tropospheric pathway through the North Pacific as well as the stratospheric pathway are fully developed. Therefore, here we mainly focus on the canonical winter response (DJF). We have now emphasized this in the introduction as well as in the discussion (lines 74-80 and 520-522).

2. Please be more consistent in the use of “linearity” and “asymmetry”. I would suggest referring to “linearity” when you describe the dependence of the response on the magnitude of an ENSO event within the same phase (El Niño o La Niña), whereas when talking about

asymmetry you compare the response to El Niño to the response to La Niña and assess whether the response to each ENSO phase is similar but opposite in sign. For example, Figures 5a) and b) shows asymmetry whereas Figures 5c) and d) shows nonlinearity.

We thank the reviewer for this comment. Because in general an asymmetry can be considered a specific type of nonlinearity we sometimes use nonlinearity as a general term in the text, including both asymmetry and single phase linearity. However, we agree with the reviewer that this can sometimes be a bit confusing and thus we have now made this distinction whenever possible throughout the text (see mainly section 4).

specific comments:

Lines 27-35 - For the non-expert reader it might help to include here a brief synopsis of what we know about the observed surface climate response to ENSO in Eurasia (temperature, precipitation).

Thanks, we have added a sentence in this regard (see lines 29-31).

Line 28 - Suggest adding reference (e.g. Li and Lau 2012) Li, Y., and N.-C. Lau, 2012: Impact of ENSO on the atmospheric variability over the North Atlantic in late winter. The role of transient eddies. J. Climate, 25, 320–342, <https://doi.org/10.1175/JCLI-D-11-00037.1>

Thank you for the suggestion. We have now included this reference.

Line 30 - I think Bell et al. (2009) were earlier than these papers to distinguish the role of stratospheric and tropospheric pathways using experiments similar to those presented in this manuscript. I therefore suggest replacing these references or at least adding Bell et al. (2009).

Thank you for noting this. We agree and therefore we have now included this reference.

Line 37 - Again, Bell et al. (2009) showed the influence of El Niño on SSWs before this paper. This reference has been included in this line.

Line 39 - Please keep the same methodology to determine the order of your citations, e.g. alphabetical, chronological or by degree of importance for supporting the previous sentence.

We have now tried to be consistent and ordered the in-text citations by degree of importance and when they have equal importance we have ordered them chronologically.

Line 42 - You can reference here Table 2 of Trascasa-Castro et al. (2019) who provide a meta-analysis of studies of SSW changes under ENSO.

We have now added a reference to Table 2 of Trascasa-Castro et al. (2019), which we agree that fits here very well.

Line 43 - “longer time series” is vague - longer than what? The current reanalyses? What would constitute “long enough”?

We mean longer than the current reanalysis. We have now clarified this in the text.

Line 55 - Also Bell et al. (2009). Note also that Toniazzo and Scaife (2006) used a model that couldn't reproduce the stratospheric pathway of ENSO to the North Atlantic. A more recent

reference that reaches a similar conclusion using a well resolved stratosphere model is Hardiman et al. (2019): Hardiman, S. C., Dunstone, N. J., Scaife, A. A., Smith, D. M., Ineson, S., Lim, J., Fereday, D. (2019). The impact of strong El Niño and La Niña events on the North Atlantic. *Geophysical Research Letters*, 46, 2874– 2883. <https://doi.org/10.1029/2018GL081776>

We have added these two references in the mentioned sentence.

Line 60 - To distinguish from subtropical jet suggest: tropospheric = eddy-driven.

Thanks for the suggestion, we now refer to the tropospheric eddy driven jet.

Lines 116-118 - I suggest strengthening the argument for why you impose opposite in sign but identical spatial pattern of SST anomalies. Garfinkel et al. (2018=the salience of nonlinearities...) suggested that the location of SST anomalies have a large influence, but as you said in Jimenez-Estevé and Domeisen (2019) the magnitude has a larger effect on the teleconnection than the spatial location of SSTs, and that's what you want to know.

Due to the design of the model experiments we isolate the nonlinearities and asymmetries originating only in the magnitude of the ENSO forcing, while removing the effect of the longitudinal location and asymmetry in the observed SST ENSO anomalies. However, we cannot say that the magnitude has a larger effect than the longitudinal location in causing such nonlinearities, but that these can originate solely due to the ENSO magnitude. In the real world, nonlinearities/asymmetries likely arise as a combination of these two factors (location and strength). Answering the question of which factor might be more important does not have a simple or a direct answer as these tend to be linked in the real world. In our study we focus on the nonlinearity/asymmetry of the response with respect the magnitude of the tropical forcing and therefore we cannot quantify if this is more or less important than the nonlinearities due to the location of the SST forcing. We have now clarified this in the methods section (lines 131-134).

Lines 134-136 - A bit more on how the nudging affects the tropospheric variability changes (or not) in the set-up used here would be helpful as compared to the control model. e.g., are there changes to the major modes of variability that go on to be assessed (e.g., amplitude of the NAO) and/or the tropospheric jet decorrelation timescale?

Now we provide additional information about how the stratospheric nudging affects the tropospheric variability, which differs from our previous study Jiménez-Estevé and Domeisen (2019) which analyses the nonlinearity in the North Pacific sector but not using nudging.

In the nudging simulations employed in the present study, the interannual winter (DJF) NAO variance decreases by 40% with respect to the 5 identical simulations when the nudging is not applied. In the North Pacific, the effect of the nudging is much weaker than in the North Atlantic, and the Aleutian low variance decreases only by 10% when the nudging is applied. However, the applied stratospheric nudging does not lead to any significant circulation anomalies in the tropospheric mean flow and the main modes of variability (EOF based) in the North Atlantic remain unaltered. Therefore we concluded that the nudging technique is very useful to isolate the tropospheric pathway while it clearly removes the stratospheric pathway in the model simulations. This is shown in the new supplementary figure S3, which displays the first

two EOFs of the winter SLP in North Atlantic region for the JRA-55 reanalysis and for the model simulations with and without a nudged stratosphere. See changes in lines 152-159 in the annotated manuscript.

Line 183 - In agreement with Bell et al. (2009), Cagnazzo and Manzini (2009).

We think these references are not needed here, the Aleutian low response to ENSO is a common feature reported in most of the cited studies in the introduction. These references are cited in several other places in our study.

Line 186 - Is stronger than “is more than” and covers a larger area. That’s really asymmetry rather than nonlinearity.

We have changed this sentence to “is stronger and covers a larger area than” and referred to it as an asymmetry instead of a nonlinearity.

Line 186 - Refer to Figure 5 as well as to Figure 2d.

Thanks. We have included the reference to figure 5.

Line 192 - I don’t see negative SLP anomalies in the North Atlantic as a response to moderate El Niño. I would rather say that moderate El Niño events only affect the Northern lobe of the NAO by leading to positive SLP anomalies of similar magnitude to strong El Niños. The SLP pattern shown in this work for strong El Niño (Fig. 2a) resembles the pattern shown by Toniazzo and Scaife (2006) in figure a20, correspondent to the El Niño event of 1998 which had a Niño3 SST anomaly of 2.7 K. Out of 20 events they examine, this is the only situation where positive SLP anomalies in the North Atlantic extend to Europe and negative SLP anomalies dominate in the southern lobe of the NAO (weakening the Azores high).

We agree with the point of the reviewer and thus we have changed the following sentence in line 216: “the moderate EN forcing only leads to a significant response in the Northern lobe of the NAO, i.e. the Icelandic low, with an insignificant impact on the Azores high.”. Furthermore we also added a reference to the Figure 2 in Toniazzo and Scaife (2006) and the similarity between the strong EN response and the 1998 EN event.

Lines 194-5 - A more detailed comparison of Figure 2a and 2b with Bell et al (2009) Figure 10 and Figure 11 middle right and lower right panels would also be helpful here as their experiments are for moderate and strong El Niño forcing with a degraded and relaxed stratosphere. There are some differences in your results, for example the location of the positive SLP anomaly in the North Atlantic in the moderate EN case; it would be instructive to the reader to discuss these more carefully as the comparison is very similar to your experiments.

Thanks for pointing this out. We have added a few sentences in this paragraph to compare also the different response for moderate events in the two studies (lines 222-225). We think that this difference might be explained so to differences in the SST forcing. The forcing used in Bell et al. (2009) for EN is based on the average of the four strongest EN events. That leads to a forcing peaking above 2K in DJF which is stronger than the 1.5K imposed in our moderate EN simulations. This difference in the magnitude likely explains why their moderate EN response

pattern looks more like the strong EN response, just weaker in magnitude.

Lines 208-220 - For a "pure" NAO- signal, one would expect the low-level Atlantic jet to shift south. For the experiment with the strongest projection onto NAO-, the strong EN case, the jet weakens rather than shifts (Fig 3a). For the weaker projections onto the NAO in the moderate EN and LN experiments the NA jet shows more of a shift. It therefore seems that the NAO does not fully explain the NA jet behaviour and low-level temperature patterns in the simulations. Have you thought about examining the East Atlantic pattern to see whether the response projects onto that mode (Figure 2b)?

We do not claim that the strong EN response "only" projects on the "pure" NAO-, and neither do the other three ENSO SLP responses. At lower levels the negative phase of the NAO can be in general both associated to a south shift and to a weakening of the zonal winds. See for example the Figure 11 in Woollings et al. (2010). This figure also shows that to fully describe the speed and latitudinal location of the North Atlantic low level eddy-driven jet, the NAO and the EA have to be used in combination. According to this same figure a weakening of the low level jet would correspond to a negative phase of the EA pattern. We now mention that the response for EN likely also projects onto the EA pattern (lines 249-250)

It also seems (**lines 216-219**) you are saying that the response is not barotropic, whereas a pure internally generated NAO signal would typically shown an equivalent barotropic structure. Relevant to this point is the study by Mezzina et al (2020) so I suggest you include that as part of this discussion: Mezzina, B., J. García-Serrano, I. Bladé, and F. Kucharski, 2020: Dynamics of the ENSO Teleconnection and NAO Variability in the North Atlantic–European Late Winter. *J. Climate*, 33, 907–923, <https://doi.org/10.1175/JCLI-D-19-0192.1>

We do not explicitly say that the response it not barotropic. In fact, we say it is mostly barotropic when comparing the geopotential and SLP response (see line 230). Nevertheless, we thank the reviewer for the suggested reference and we now cite Mezzina et al. (2020) in line 252 to say that a purely internally generated NAO would have a more barotropic structure.

Line 216 - Only a weak strengthening for La Niña.

We have now emphasized that the response for La Niña is weak.

Line 216 - Line 220 - Add references: Ineson and Scaife (2009), Cagnazzo and Manzini (2009). In these lines we are explicitly referring to the result shown by Madonna et al. (2019) that the North Atlantic jet is more thermally driven during El Niño.

Lines 223-225 - "For example, the weaker baroclinicity during strong EN tends to weaken the climatological Icelandic low, whereas the strengthening of the meridional temperature gradient during LN can be linked to the intensification of the Icelandic low and the associated near surface westerly winds (Figure 3c,d)." There is some nonlinearity here between baroclinicity anomalies over North America and the strength of the Icelandic low: For that specific low pressure system, and ignoring now the Azores high, baroclinicity anomalies are double in magnitude in strong ENSO events, whereas the strength of the Icelandic low seems the same in the moderate and

strong events. Why is that?

We agree with the reviewer that the relationship between baroclinicity and the Icelandic low pressure anomaly seems to be nonlinear. The relationship between these two magnitudes is rather complicated, it is therefore very difficult to infer any causality from just these two plots. Because there are different mechanisms involved in the tropospheric pathway, it can be that there is a compensation between the baroclinicity mechanism and the changes in the horizontal WAF for LN. In this regard, we have added some discussion in lines 315-319 saying that the nonlinearity within the LN phase seems to be explained through the nonlinear response of the quasi-stationary eastward WAF (see the pdfs in the old Figure 8f, now figure 9f).

Line 255 - Wave train pattern in figure 5a? Is a Rossby wave source anomaly plot necessary to identify possible sources in the Caribbean that might explain this NAO pattern?

As the reviewer points out, the asymmetry pattern in Figure 5a might be related to an asymmetry of the Rossby wave source (RWS) response in the Caribbean. In this regard, we have now included the Rossby wave source response for the 4 sensitivity experiments (Figure S1 in the supplementary). In Figure S1 an asymmetry between moderate EN and LN in the Caribbean-Tropical North Atlantic RWS is observed, which could be one of the factors together with the lack of a significant eastward transient WAF for the moderate EN simulation, explaining the wave-pattern in the North Atlantic SLP asymmetry for moderate events. This discussion has been now included in this section of paper (see lines 290-293)

Line 258 - There are other mechanisms through which ENSO can affect the NAO besides the one proposed in this study. In order to be able to explain the anomalous winds and temperature anomalies associated with both moderate and especially strong El Niño events, more analysis is necessary. I would suggest to plot Rossby wave source anomalies as well as SLP response by months to look for a non-stationary NAO response.

We now included the mean DJF Rossby wave source response in the new supplementary Figure S1 and refer to it in the text (see answer to the reviewer comment above). The focus of the present paper is to characterize the canonical mid winter response (therefore we use DJF means for most of the analysis). Nonetheless, we have also checked the monthly evolution of the SLP response for each of the ENSO forced simulations, and we find that the response in the North Atlantic is strongest in December-January despite the strongest response in the North Pacific occurring in January-February. The weaker response in late winter might be explained due to the lack of the stratospheric pathway in the model experiments. We think the current simulation setup is not adequate to provide further detail on the intra-seasonal evolution, as this is missing important ingredients, like the remote SST anomalies in the tropical North Atlantic and North Pacific, and the stratospheric pathway. For this purpose a more complex model would be also desired and this is not the focus of the present study. This is highlighted in 284-285.

Garcia Serrano (2017) (<https://doi.org/10.1175/JCLI-D-16-0641.1>) studies the lagged ENSO-Tropical North Atlantic relationship which consists on a Gill-type response associated with a perturbed Walker Circulation. In your experiments SST are fixed so you cannot look at a

lagged SST response in the TNA but you could look at the lagged SLP response in the North Atlantic, month by month as in Bell et al (2009) or Trascasa-Castro et al (2019) to see if there is any differences in the SLP response in the North Atlantic in late winter that might suggest an influence of the ENSO-TNA teleconnection as well as the ENSO-PNA teleconnection that you have described in your article.

The lagged response of the Aleutian low SLP in the model is analysed in (Jiménez-Esteve and Domeisen, 2019). As mentioned above, the model experiments are too idealized to reproduce the lagged response in the North Atlantic. Differences between early and mid-to-late winter are not statistically different when considering the strong interannual variability in the North Atlantic circulation. Therefore to avoid confusion we decide to mainly focus on the winter averaged response.

Line 268 - Those studies suggest the dominance of the tropospheric pathway for strong EN is due to a saturation of the stratospheric pathway. However, in Hardiman et al (2019) their weak El Nino case shows a less active stratospheric pathway than observations which may highlight as issue with their approach. Trascasa-Castro et al (2019) showed the stratospheric pathway may not saturate for strong EN and hence there is still some debate around the proposed "saturation mechanism" which you should mention here.

In the mentioned line we do not refer to the saturation of the stratospheric pathway because our model simulation exclude this mechanism by construction. According to our experiments the nonlinearity pattern observed in Figure 5a,c may also originate due to the competition between different nonlinear tropospheric 'pathways' or mechanisms, for example the Caribbean Rossby wave source and the downstream zonal wave propagation from the Pacific. We have now clarified this in lines 311-314.

Line 277 - I think this is a non-standard definition of the NAO index (neither station based nor EOF based). What are the implications of averaging over such a large area to calculate the NAO index rather than using Iceland and Azores?

Averaging over a specific geographical area is a common approach in several modelling studies (e.g., Li and Wang, 2003; Stephenson et al., 2006; Zhang et al., 2019). Using an area average is better than using a point based index, as in model the centers of action might be slightly shifted with respect to observations. In addition, using EOFs to define the NAO variability leads to comparable results as is remarked in the text (line 348). We prefer to stick to the current definition as it is also more consistent to the Aleutian low definition and it allows us to divide the NAO into an Icelandic low and Azores high contribution. Figure S3 also shows the NAO pattern obtained using the EOF analysis and we can see that the pattern is identical to the one obtained using the averaged SLP difference between the Icelandic low and Azores high boxes (Figure 8).

Line 279 - Difficult to compare these (DJFM) with Fig 2 (DJF)

We use monthly instead of seasonal anomalies as these better represent the sub-seasonal timescales on which these pressure systems vary, but using seasonal means leads to comparable results. This

allows us to also increase the sample size by a factor of 4, which enables us to obtain a better estimation of the respective PDFs. Find below the comparison between PDFs of the AL and the NAO using winter months and DJF means instead. Note that the results remain the same despite having a stronger signal in the DJF mean (color ticks along the x-axis).

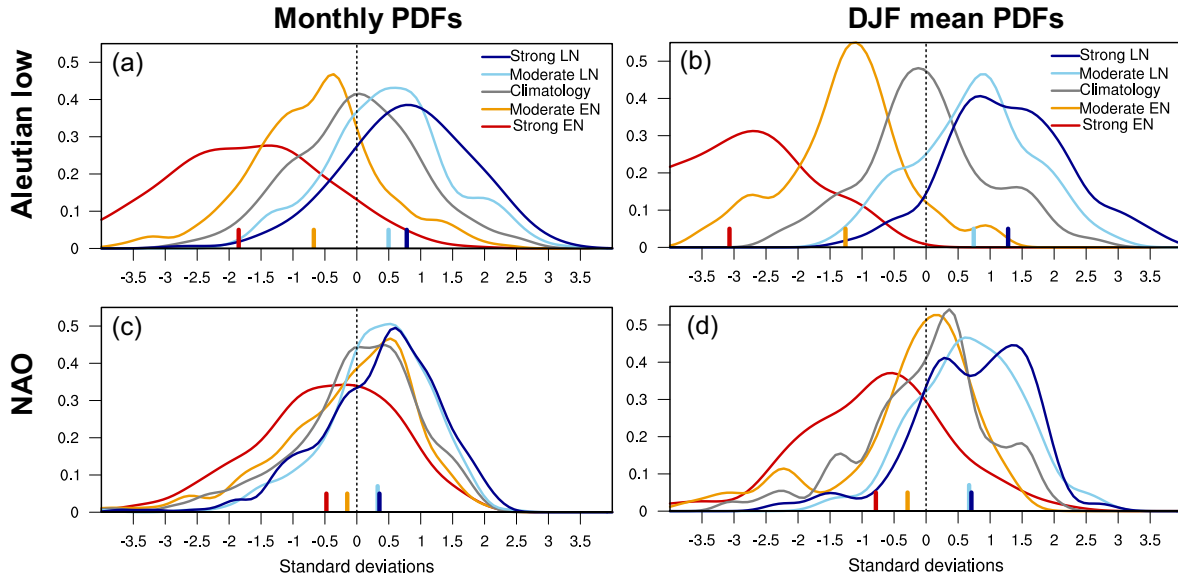


Figure R1: The PDFs of the December-January-February-March standardized monthly means for (a) the AL and (c) the NAO indices. (b,d) the same but using DJF seasonal means instead. Colors represent the PDFs for the different ENSO forcings (red: strong EN, orange: moderate EN, grey: climatology, light blue: moderate LN, dark blue: strong LN).

Lines 291-292 - I see what you are talking about, but is it partly a plotting issue? The amplitude of North Atlantic anomalies in Fig 6a is smaller than in 6b and you white out values $< |0.5|$ hPa. If you add another contour does the dipole appear to extend further to Europe?

This is not a plotting issue, we have tried to add another contour and the dipole does not extend further much into Europe. The point we want to make here is that the influence of the AL over Europe is weaker because it is indirect, as compared to the more direct impact of the NAO.

Lines 294-295 - Can you comment on whether there are changes to the shapes of the pdfs? It appears there might be so you could mention higher order moments than the mean if the differences are significant.

We have now plotted a new figure S4, where the values of the 3 first moments (mean, standard deviation and skewness) are compared for the 5 simulations and for the AL and NAO monthly PDFs. A part from the already commented nonlinearity in the average response, we find that EN (LN) tends to increase (decrease) the standard deviation of both the AL and the NAO. A clear conclusion cannot be obtained for the skewness parameter, but we find that in general a strong EN decreases the negative skewness of the climatological NAO and makes the pdf more symmetric, similar to the AL. This Figure is now shown in the supplementary material, while in the manuscript we mention the previous observations. However, we do not have a clear

explanation for this higher momentum changes.

Line 293 - These other mechanisms could include the stratosphere but also the tropical Atlantic pathway; more analysis is needed to fully explain the positive SLP anomaly over Europe.

We agree with the reviewer that other mechanisms have to be included to account for the full observed response over Europe. The tropical Atlantic contribution is not fully removed from this analysis, as the Aleutian low and the Rossby wave source in the Caribbean are themselves linked through the common ENSO forcing, while the stratospheric pathway is fully removed in our model experiments. We have now clarified this point in the text (see lines 311-314).

Line 303 - I don't agree that Fig 2b) shows that moderate EN projects onto a negative phase of the NAO. It might weakly project onto the NAO index as defined here, but it also looks like a blocking pattern.

We agree with the reviewer that the moderate EN projects weakly on the negative NAO and that the response might project stronger on the East Atlantic pattern. However, in this section we address the linearity in the projection on the NAO pattern and thus introducing another index would complicate the interpretation of the results. Nevertheless, we have included a sentence on the text which says that the moderate EN in fact projects strongly on the second mode of variability in the North Atlantic sector.

Line 307 - Response might be lagged.

This does not seem to be the case, as we use individual standardized monthly values. Moreover, the fact that the negative skewness of the NAO is reproduced in the model is another prove that the model correctly reproduces the observed NAO variability.

Line 314 - Is it remarkable? You did run the model for 80 years to get a high signal-to-noise ratio!

The variability of the NAO and the ENSO signal (thus the signal-to-noise ratio) do not vary with longer simulation times as this are intrinsic properties of the system. Due to the large internal variability of the NAO a large sample size is needed to obtain a significant correlation and that is what we did. In summary, while the long simulations make it possible to get a statistical robust value of the slope of the regression, that does not change the value of the slope. What we referred as to remarkable was the value of the slope, but we agree that the sentence is confusing and we have removed the statement.

Line 316 - Trascasa-Castro et al. (2019) also show this result for the NAO so please add citation.

This citation has been added.

Lines 400-410 - While this synthesis of studies is useful some key points are missing: - Hardiman et al (2019) use ensemble of seasonal hindcasts, so the experiments are initialised and are individual ensemble members for only a few observed ENSO cases. This is a very different approach to the other atmospheric model studies described so is worth highlighting.

- Rao and Ren (2016a) uses observations so is beset by small sample sizes, as you highlight as

an issue on line 77

- Weinberger et al (2019) use experiments with observed SSTs so their results capture differences in ENSO magnitude and pattern while this study, Rao and Ren (2016b) and Trascasa-Castro et al (2019) remove differences in pattern through an idealised experiment design.

We thank the reviewer for the above suggested points. We have now included this information points into the discussion section.

Lines 412-413 - Also likely to be important for determining how important the tropospheric and stratospheric pathways are would be the model's climatology in the stratosphere, e.g. Bell et al (2009) used a model with relatively few SSWs and Toniazzo and Scaife (2006) used a low top model with weak stratospheric variability.

We also added the variability of the stratosphere as a factor to consider (line 499)

Lines 432 - Add reference Rodriguez-Fonseca et al. (2016).

Thanks. We added this reference.

Lines 433 - Again mention this relies on a saturation of the stratospheric pathway for strong EN and it is still an open research issue as to whether this would occur. Even if the stratospheric pathway saturates at some point, its effect should no disappear altogether at strong EN as the results of Bell et al (2009) in their damped stratosphere case suggest.

We now mention the saturation of the stratospheric pathway as a necessary condition for this result.

Technical Corrections:

Line 17 - Define SST acronym in main text [changed](#)

Line 44 - "On average, Arctic stratospheric anomalies ..." [changed](#)

Line 59 - lead = leads [changed](#)

Line 74 - Therefore, the tropospheric pathway for ENSO impact [changed](#)

Line 152 - Previous = prior [changed](#)

Line 201 - Remove "do" [changed](#)

Line 314-315 - Remove "Figure 7 also serves to illustrate the large internal variability in the extratropics" = repeated sentence. [We modified the sentence](#)

Line 321 - dominantly = predominantly [changed](#)

Line 401-402 - Replace "an state-of-the-art seasonal prediction model" with "atmospheric model" – the model is HadGEM3 which is in the same family as GloSea5 but run in a different configuration. [changed](#)

Reviewer 3:

This paper analyzes the tropospheric impacts of ENSO on the North Atlantic region, focusing on nonlinearities regarding the amplitudes of the events, and asymmetries comparing El Niño and La Niña phases. To do so, they use different idealized simulations with a simplified model in which stratospheric winds are nudged to climatological values to shut down the stratospheric ENSO pathway.

We thank the reviewer for their comments on our manuscript, which have helped to improve this study. We answer point by point to the comments below.

General comments:

1. This study extends that from Jimenez-Esteve and Domeisen (2019) who studied the nonlinearities of the ENSO teleconnections to the North Pacific. The authors use similar idealized experiments in both papers except that they shut down the stratospheric pathway by nudging the stratospheric winds to the climatology in the present study. For the readers interest, it would have been easier to have one single paper on the asymmetries of the tropospheric ENSO pathway and make the paper more self consistent and not having the reader go back and forth between papers. I detail below some of my concerns with comments to improve the paper, making it more self consistent and complete.

Initially, as the reviewer suggests, we thought of publishing a paper with the results of the current paper and Jiménez-Esteve and Domeisen (2019) together. However, due to the quantity of interesting results and the different physical mechanisms in the North Pacific, we decided to split up the material into a paper focusing in the nonlinearity and asymmetry in the North Pacific and a more extensive paper focusing on the tropospheric pathway to the North Atlantic. Nonetheless, because the North Atlantic response to ENSO is influenced by the pathway through the North Pacific, we also have to refer to the response in the North Pacific in the current paper to explain the results here.

2. Thus, I think the paper is appropriate for publication in Weather and Climate Dynamics after the authors address the comments below. I feel the discussion of mechanisms on the origins of the asymmetries, etc, is reduced to references to Jimenez-Esteve and Domeisen (2019). This is why in a few places I ask the authors to add more information to clarify certain aspects in addition to their reference to Jimenez-Esteve and Domeisen (2019). There are many references to Jimenez-Esteve and Domeisen (2019) but results from both papers are not really compared or discussed. Indeed, the comparison of the results could give us additional information not discussed in this study.

We agree with the reviewer that we reference to our previous paper quite often in the current manuscript. This is of course mostly necessary as both studies use the same experiment design and similar methodology, and therefore it is easier and necessary to compare the results between these two studies. To facilitate the comparison between the two papers, we have added further

discussion comparing the model results, mainly in section 4, where the influence of the nudging of the stratosphere on the nonlinearities and asymmetries can be compared (see answer to the comments below).

3. The differences in the North Pacific between simulations in Jimenez-Esteve and Domeisen (2019) and the present manuscript must be related to the stratosphere (e.g. comparison of Figs. 2 and 5 in both papers). These differences and possible explanations should be discussed further not only in the Pacific (as it is done in Jimenez-Esteve and Domeisen (2019)) but also in the Atlantic. I also recommend plotting fig. 5 in the same projection as in Jimenez-Esteve and Domeisen (2019) for easy comparison. I see differences in the Atlantic region already comparing Fig.5 of both papers that need to be discussed.

To facilitate the comparison, we have now re-plotted figure 5 using a stereographic projection as in figure 5 in Jiménez-Esteve and Domeisen (2019). We can now see that most of the differences are localized in the North Atlantic, where the influence of stratospheric nudging is more relevant, while the nonlinearities in the North Pacific are similar for both plots. These differences are now mentioned in section 4

4. As figure 4 in Jimenez-Esteve and Domeisen (2019) compared their modeling results to reanalysis data, here a similar comparison should be made when possible, Figure 2 to 4 (or some of them) from Section 3 and figures 5 and 7 for asymmetries. Similarities and differences between model and reanalysis would give hints about how realistic are the modeling results when comparing the signals in the Pacific and about the relative role of the tropospheric and stratospheric pathways when comparing the signals in the Atlantic Ocean.

We agree with the reviewer that further comparison with reanalysis would ideally help. However, in Jiménez-Esteve and Domeisen (2019) it was already challenging to clearly compare the model results with observations, as very few strong ENSO events have been observed. This comparison becomes extremely challenging or impossible when analysing to the North Atlantic response in our model experiments, as the reviewer also points the 3 strongest EN events coincided with a stronger than normal stratospheric polar vortex (see for example Figure 3b,d in Hardiman et al. (2019)) and therefore we cannot conclude anything about the tropospheric pathway for strong events using simple composite techniques and reanalysis as these might also contain the anomalous stratospheric influence. Furthermore, as it is already discussed in the paper, there is still a big debate around the linearity in the stratospheric pathway in models and observations (Weinberger et al., 2019; Hardiman et al., 2019; Trascasa-Castro et al., 2019) and therefore we focus here on isolating the nonlinearity in the tropospheric pathway, which unfortunately can only be done using model simulations and not using reanalysis.

To show our point, below the JRA-55 reanalysis (Kobayashi et al., 2015) DJF SLP anomalies are plotted for the ENSO events of different magnitude. In this Figure shows that while in the North Pacific the response agrees quite well with model results, in the North Atlantic the response is different for the strongest events, and it projects onto the positive NAO phase, probably due to a destructive interference with the strong polar vortex observed during these events.

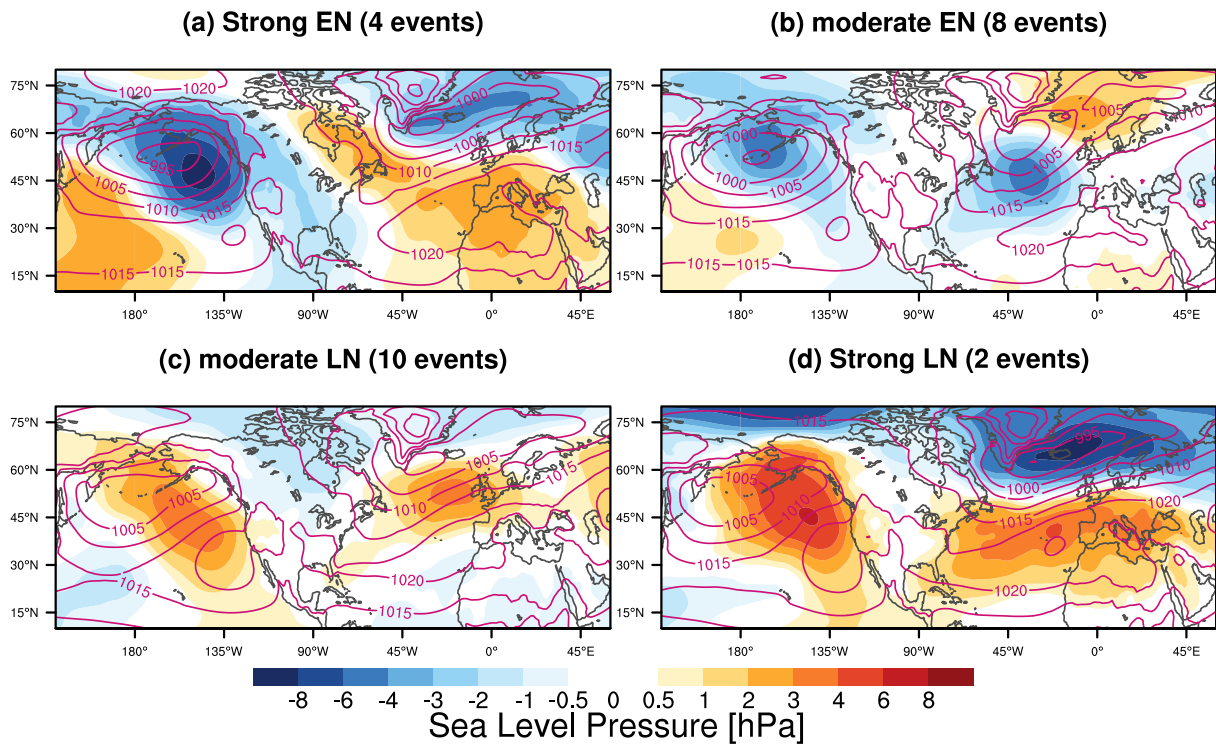


Figure R2: JRA-55 reanalysis (1958-2016) JFM mean SLP anomalies (in hPa) averaged over the (a) 4 strongest EN events (ONDJF Nino3.4 > 2 stddev.), (b) 8 moderate EN events (2 stddev. > ONDJF Nino3.4 > 1 stddev.), (c) 10 moderate LN events (-2 stddev. < ONDJF Nino3.4 < -1 stddev.), and (d) the 2 strongest LN events (ONDJF Nino3.4 < -2 stddev.). Solid contours display the total averaged field.

In the case of figure 7 (now figure 8), we have tried to repeat the same analysis but using the JRA-55 reanalysis. This Figure now is shown in the supplementary material, as it is not really comparable to Figure 8. The figure shows a weaker and non-robust correlation between the DJF mean AL and the NAO indices. This might be due to the small sample size for strong ENSO events and the stratospheric influence, whose effect is removed on purpose in our model simulations. We refer to this result as well as to the explanation for the discrepancy in the main text (lines 391-395).

5. Several studies have pointed out differences in the timing of the teleconnections in the Pacific and Atlantic Oceans (e.g. early vs late winter). How different are the responses and the nonlinearities and asymmetries if we look at individual months or early vs late winter instead of DJF means? No need to show figures but add a sentence in the manuscript.

We have analysed the winter monthly evolution of the response (November to March) and find that the response in the North Atlantic peaks around December-January depending on the simulation. In terms of its pattern the SLP and geopotential height response does not show significant intra-seasonal variations and remains similar to the averaged DJF response. The weaker response in late winter compared to reanalysis might be explained due to the lack of the stratospheric pathway in the model experiments. Therefore, we think that the current

simulation setup is not adequate to provide further detail on the intra-seasonal evolution, as this are missing important ingredients, like the remote SST anomalies in the tropical North Atlantic and the stratospheric pathway, the latter might be more important in late winter. For this purpose a more complex model would be desired and this is not the focus of the present study. This is now mentioned in the article (lines 284-285 and 521-522)

6. Regarding wording, I find confusing the use of ‘nonlinearity’ in certain places particularly in relation to ‘asymmetry’. I recommend using nonlinearity for differences in the response regarding the magnitude of the events, and asymmetry for the differences between ENSO phases. Indeed, this is the way it was used in Fig. 5 in Jimenez-Esteve and Domeisen (2019) while here it is not. I find this confusing

We have now made figure 5 similar to figure 5 in Jiménez-Esteve and Domeisen (2019). See also response to reviewer 2: "Because in general an asymmetry can be considered a specific type of nonlinearity we sometimes use nonlinearity as a general term in the text, including both asymmetry and single phase linearity. However, we agree with the reviewer that this can sometimes be a bit confusing and thus we have now made this distinction whenever possible throughout the text"

Minor comments:

L. 30. I believe Bell et al. (2009), Cagnazzo and Manzini (2009) and Ineson and Scaife (2009) are the first ones to discuss the stratospheric pathway in connection to North Atlantic surface impacts. Please add the references.

Thanks for pointing this out. We have now included them in this line.

L.35-50. All this paragraph reads too long considering that the stratosphere is not the main focus of the study. I would shorten it and move it to line 75 to connect to the paragraph previous to the last one of this section.

Thank you for pointing this out, this paragraph has been shortened.

L. 53-L.70. The description of mechanisms is confusing. The authors start saying that they focus on the NP downstream effect. Which one is that of the ones described later on? Perhaps listing then as first, second, etc would help.

We agree with the reviewer that the beginning of the paragraph was a bit misleading. We have now listed and clarified the explanation of the tropospheric mechanisms.

L. 71-75. Which one is the mechanism used in the study?

We have now added the following sentence: "We focus on the effect of the changes in the total eastward wave activity fluxes of transient and QS waves, and the baroclinicity mechanism. However, nonlinearities in the North Atlantic response to ENSO are better explained in terms of the former mechanism."

L.107. Please remove ‘As in Jimenez-Esteve and Domeisen (2019)’.. it adds confusion.

Removed

L.111. When mentioning here the four spatial patterns, please refer to figure 1a.

Thanks, we have added now this reference.

L. 177. This first sentence is not very clear. Indeed the authors analyze these simulations throughout the paper. So the sentence can be improved to focus more on this particular section. Please substitute ‘while relaxing. . .’ by ‘by relaxing . . .’

Changed ‘by relaxing’.

L.180. Here and throughout the paper, are the results similar if we look at individual winter months instead of DJF averages? Do we see differences between early and late winter in the teleconnection and asymmetries? (see my general comments above).

Yes, there are some small differences when looking at individual months. This is due to the fact that the peak of the response varies slightly between the different forcing experiments, December or January. However, the teleconnection patterns remain similar (see answer to the previous comments). To avoid confusion and unnecessary detail, in the manuscript we prefer to keep using DJF means to analyse the asymmetry and nonlinearity. This is stated now at the beginning of section 4.

L.185 Following my comment about asymmetries vs linearity above, I think asymmetry should be used here.

Thanks, we now use here the term asymmetry.

L. 232. Can the authors argue about why the response in temperature in EN over Europe is the opposite from a negative NAO? However, for LN the response is as expected, right?

This is because, although EN projecting on a negative NAO, the pattern does not extend over the European continent as the full pattern of the NAO. Instead we find that positive geopotential anomalies occur over Europe during strong EN (Figure 2a). This leads to a warm air advection from the warmer North Atlantic ocean (Figure 3a). See lines 264-266.

Section 4 . Perhaps the title would be more appropriate as ‘Spatial distribution of the asymmetry and non-linearity response to the ENSO. . .’ or something similar. For a better comparison with Jimenez-Esteve and Domeisen (2019) please replot the figure with the same polar projection and add the same ‘phase asymmetry’ and ‘single phase nonlinearity’ to the figure.

We have changed the title to: “Spatial pattern and statistical robustness of the nonlinear and asymmetric North Atlantic response to ENSO forcing”. This section has substantially changed following the recommendation of reviewer 1, we now analyse the robustness of the observed patterns (see new figure 6). Also following the reviewer suggestion, we replotted Figure 5 accordingly.

L. 254. Where do we see in Fig. 5 that the asymmetry denotes a stronger AL/PNA for moderate EN than moderate LN? Individual phases are not shown here.

We do not show individual phases here, but the sum of the EN and LN response. The above conclusion is obtained by comparing figure 2b and 2c. Because the AL response to moderate EN is negative and the response to moderate LN is positive, the negative sign over the AL region

in the asymmetry plot denotes a stronger impact during moderate EN. We have clarified this in the text (line 290).

L. 257 ‘EN compared to LN (not shown), and the strong . . .’

It is shown in Figure 2a,d. We now refer to this figure in the text.

L.266 Note also than in observations, the strongest EN winters are not accompanied by SSWs. Yes, we are aware of this and now we also mention this in the text (line 313).

L.270. Note that the impact over Europe is linear (there is no signal in figure 5d). However, there is some positive signal in Fig. 5d in Jimenez-Esteve and Domeisen (2019), does this mean that the non linearity in that case came from the stratosphere? This is the type of comparison/discussion that needs to be included.

We do not see significant differences between figure 5d in this paper and 5d in Jimenez-Esteve and Domeisen (2019). The most evident differences are between Figures 5a,b between the two papers, i.e. the asymmetry. In this case we agree with the reviewer that the differences in the asymmetric response have to be linked to the differences in the stratospheric response. We mention this in lines 298-301 of the new version of the manuscript. However, because the employed model is not able to reproduce a very ‘realistic’ stratospheric pathway as in reanalysis a detailed interpretation between the two studies might be affected by the mentioned model ‘bias’. Nonetheless we think than the model results in this study can be trusted when removing the stratospheric influence (figure 5).

L.298. and paragraph above. Can perhaps the authors explain a bit more about the origin of the nonlinearities (mechanism) here?

The convective response to the underlying SST is nonlinear mainly for large SST forcings in the tropical Pacific (see Figure 4 in Jiménez-Esteve and Domeisen (2019)). This is due to a threshold behavior for the occurrence of deep convection (e.g. Johnson and Kosaka, 2016). We have clarified this in the text while also adding the above reference.

L. 312. Can the authors include reanalysis data in Figure 7? Similar to the scatterplots in fig. 4 of Jimenez-Esteve and Domeisen (2019)? The comparison would give us a hint also on the role of the stratosphere.

This is a good suggestion. We have plotted a similar Figure 7, but using the JRA-55 reanalysis. These results are now shown as a supplementary Figure S5, because the two figures are not really comparable due to the lack of the stratospheric influence. The figure shows a weaker and non-robust correlation between the DJF mean AL and the NAO indices. This might be due to the small sample size for strong ENSO events and the stratospheric influence which is on purpose removed in our model simulations. We refer to this result as well as to the explanation for the discrepancy in the main text (lines 391-394)

L. 319. Fig.4 in Jimenez-Esteve and Domeisen (2019) do not show convection directly. Can the authors elaborate their argument a bit more here?

Figure 4 in Jiménez-Esteve and Domeisen (2019) shows the central Pacific poleward divergent

wind at 150hPa with respect to the NINO3.4 SST anomalies. This is a direct measure of the dynamical response within the tropics. Another reason to use divergent winds instead of OLR for example is because our model does not simulate clouds. Nevertheless, divergence at the upper troposphere in the tropics is very closely linked to the deep tropical convection. We have rewritten this sentence to clarify our reasoning.

L. 385. I also see a dipole for strong LN in Fig. 2d.

Yes, we agree with the reviewer that there is also a dipole structure, but the conclusion that the strongest impact is located over the Icelandic low does not change.

L.388-390. I understand it might be difficult to answer, but the authors should discuss and elaborate on why moderate LN forcing has a stronger impact than moderate EN forcing or why there is a saturation effect for LN and not for EN? How all of this compares to observations? This question is indeed very difficult to answer and cannot be fully resolved in this paper, neither using reanalysis where this asymmetry is so far not present nor detectable. Using the several diagnostics in this paper we can explain the stronger projection of the moderate LN response onto the NAO due to several factors:

- Stronger QS WAF response for moderate LN than for EN (see Figure 9f) and thus a stronger impact over the Icelandic low for moderate LN.
- The moderate EN leads to a stronger Rossby wave source response in the tropical North Atlantic (Figure S1), which might be related to the observed blocking pattern (Figure 2,b), which weakly projects onto the NAO.
- The insignificant response of the transient WAF for the moderate EN (Figure 9c) leads to an insignificant response over the Azores high, thus also weakly projecting onto the NAO.

Thus it seems that while the tropospheric mechanisms linking the AL availability and the NAO during the moderate LN are stronger, during moderate EN the tropical RWS in the Caribbean leads to a blocking pattern that weakly projects onto the NAO. These points are now included in the discussion section.

L. 392. Where is the sentence ‘. . .although the stratosphere may contribute when it is active’ from?

Thanks, this part of the sentence has been removed.

L. 400-410. I find this discussion too long for something not directly related to the paper, as there is no focus on the stratospheric nonlinearities. Please make it shorter. We agree that the focus of the paper is the nonlinearities and asymmetries within the tropospheric pathway. However most of the previous literature on the North Atlantic response to ENSO consider the stratosphere as a crucial part to explain this teleconnection. Furthermore, we think that the disagreement between these studies is something that is worth mentioning in the discussion of the paper, which is one of the reasons that motivated us to exclude the stratospheric contribution

of this teleconnection. We have made an effort to shorten this paragraph, though as reviewer 2 recommends us to expand this paragraph by including several extra points, we have been working on finding a balance between these requests.

References

- Ayarzagüena, B., Ineson, S., Dunstone, N. J., Baldwin, M. P., and Scaife, A. A. (2018). Intraseasonal Effects of El Niño–Southern Oscillation on North Atlantic Climate. *J. Clim.*, 31(21):8861–8873.
- Bell, C. J., Gray, L. J., Charlton-Perez, A. J., Joshi, M. M., and Scaife, A. A. (2009). Stratospheric communication of El Niño teleconnections to European winter. *J. Clim.*, 22(15):4083–4096.
- Deser, C., Simpson, I. R., McKinnon, K. A., and Phillips, A. S. (2017). The Northern Hemisphere extratropical atmospheric circulation response to ENSO: How well do we know it and how do we evaluate models accordingly? *J. Clim.*, 30(13):5059–5082.
- Garfinkel, C. I., Weinberger, I., White, I. P., Oman, L. D., Aquila, V., and Lim, Y.-K. (2018). The salience of nonlinearities in the boreal winter response to ENSO: North Pacific and North America. *Clim. Dyn.*, 0(0):1–18.
- Hardiman, S. C., Dunstone, N. J., Scaife, A. A., Smith, D. M., Ineson, S., Lim, J., and Fereday, D. (2019). The impact of strong El Niño and La Niña events on the North Atlantic. *Geophys. Res. Lett.*
- Jiménez-Esteve, B. and Domeisen, D. I. (2019). Nonlinearity in the North Pacific atmospheric response to a linear ENSO forcing. *Geophys. Res. Lett.*, pages 1–11.
- Johnson, N. C. and Kosaka, Y. (2016). The impact of eastern equatorial Pacific convection on the diversity of boreal winter El Niño teleconnection patterns. *Clim. Dyn.*, 47(12):3737–3765.
- Kobayashi, S., Ota, Y., Harada, Y., Ebata, A., Moriya, M., Onda, H., Onogi, K., Kamahori, H., Kobayashi, C., Endo, H., Miyaoka, K., and Takahashi, K. (2015). The JRA-55 Reanalysis: General Specifications and Basic Characteristics. *J. Meteorol. Soc. Japan. Ser. II*, 93(1):5–48.
- Li, J. and Wang, J. X. (2003). A new North Atlantic Oscillation index and its variability. *Adv. Atmos. Sci.*, 20(5):661–676.

- Madonna, E., Li, C., and Wettstein, J. J. (2019). Suppressed eddy driving during southward excursions of the North Atlantic jet on synoptic to seasonal time scales. *Atmos. Sci. Lett.*, 20(9).
- Mezzina, B., García-Serrano, J., Bladé, I., and Kucharski, F. (2020). Dynamics of the ENSO Teleconnection and NAO Variability in the North Atlantic–European Late Winter. *J. Clim.*, 33(3):907–923.
- Stephenson, D. B., Pavan, V., Collins, M., Junge, M. M., and Quadrelli, R. (2006). North Atlantic Oscillation response to transient greenhouse gas forcing and the impact on European winter climate: A CMIP2 multi-model assessment. *Clim. Dyn.*, 27(4):401–420.
- Thomson, S. I. and Vallis, G. K. (2018a). Atmospheric Response to SST anomalies. Part 1: Background-state dependence, teleconnections and local effects in winter. *J. Atmos. Sci.*
- Thomson, S. I. and Vallis, G. K. (2018b). Atmospheric response to SST anomalies. Part II: Background-state dependence, teleconnections, and local effects in summer. *J. Atmos. Sci.*, 75(12):4125–4138.
- Toniazzo, T. and Scaife, A. A. (2006). The influence of ENSO on winter North Atlantic climate. *Geophys. Res. Lett.*, 33(24).
- Trascasa-Castro, P., Maycock, A. C., Scott Yiu, Y. Y., and Fletcher, J. K. (2019). On the linearity of the stratospheric and Euro-Atlantic sector response to ENSO. *J. Clim.*, pages JCLI-D-18-0746.1.
- Weinberger, I., Garfinkel, C. I., White, I. P., and Oman, L. D. (2019). The salience of nonlinearities in the boreal winter response to ENSO : Arctic stratosphere and Europe. *Clim. Dyn.*, (0123456789).
- Woollings, T., Hannachi, A., and Hoskins, B. (2010). Variability of the North Atlantic eddy-driven jet stream. *Q. J. R. Meteorol. Soc.*, 136(649):856–868.
- Zappa, G., Shaffrey, L. C., and Hodges, K. I. (2013). The ability of CMIP5 models to simulate North Atlantic extratropical cyclones. *J. Clim.*, 26(15):5379–5396.
- Zhang, W., Wang, Z., Stuecker, M. F., Turner, A. G., Jin, F. F., and Geng, X. (2019). Impact of ENSO longitudinal position on teleconnections to the NAO. *Clim. Dyn.*, 52(1-2):257–274.

Nonlinearity in the Tropospheric Pathway of ENSO to the North Atlantic

Bernat Jiménez-Esteve¹ and Daniela I.V. Domeisen¹

¹Institute for Atmospheric and Climate Science, ETH Zurich, Universitätstrasse 16, 8092 Zurich, Switzerland

Correspondence: Bernat Jiménez-Esteve (bernat.jimenez@env.ethz.ch)

Abstract. El Niño Southern Oscillation (ENSO) can exert a remote impact on North Atlantic and European (NAE) winter climate. This teleconnection is driven by the superposition and interaction of different influences, which are generally grouped into two main pathways, namely the tropospheric and stratospheric pathways. In this study, we focus on the tropospheric pathway through the North Pacific and across the North American continent. Due to the possible non-stationary behaviour and the limited time period covered by reanalysis data sets, the potential nonlinearity of this pathway remains unclear. In order to address this question, we use a simplified physics atmospheric model forced with seasonally varying prescribed sea surface temperatures (SST) following the evolution of different ENSO phases with linearly varying strength at a fixed location. To isolate the tropospheric pathway the zonal mean stratospheric winds are nudged towards the model climatology. The model experiments indicate that the tropospheric pathway of ENSO to the North Atlantic exhibits significant nonlinearity with respect to the tropical SST forcing, both in the location and amplitude of the impacts. For example, strong El Niño leads to a significantly stronger impact over the North Atlantic Oscillation (NAO) than a La Niña forcing of the same amplitude. For La Niña forcings, there is a saturation in the response, with no further increase in the NAO impact even when doubling the SST forcing, while this is not the case for El Niño. These findings may have important consequences for long-range prediction of the North Atlantic and Europe.

1 Introduction

El Niño Southern Oscillation (ENSO) is the most important mode of interannual variability in the tropical Pacific. Trade winds, sea level pressure (SLP), precipitation, and sea surface temperatures (SST)s irregularly oscillate between a warm (El Niño, EN) and cold (La Niña, LN) phase (e.g., Philander, 1990; Diaz et al., 2001). By means of Rossby wave trains, the associated tropical circulation anomalies can also influence the extratropical circulation (Hoskins and Karoly, 1981; Sardeshmukh and Hoskins, 1988; Liu and Alexander, 2007). An important ENSO teleconnection is observed during winter over the North Pacific and the North American continent (Bjerknes, 1969; Horel and Wallace, 1981; Mo and Livezey, 1986; Ropelewski and Halpert, 1987; Halpert and Ropelewski, 1992; Trenberth et al., 1998), consisting of a strengthened Aleutian low (AL) (e.g. Barnston and Livezey, 1987) and a southward shift and eastward extension of the tropospheric jet and the storm track (Seager et al., 2010) during EN, projecting on the positive phase of the Pacific North American (PNA) pattern (Wallace and Gutzler, 1981).

25 Opposite-signed anomalies tend to be observed during LN, yet there are significant nonlinearities in the location and strength of the impacts (e.g., Zhang et al., 2014; Frauen et al., 2014; Garfinkel et al., 2018; Jiménez-Esteve and Domeisen, 2019).

The North Pacific circulation anomalies associated with ENSO can influence the North Atlantic. The ENSO signal reaches the North Atlantic through different mechanisms (e.g., Brönnimann, 2007; Li and Lau, 2012a; Jiménez-Esteve and Domeisen, 2018, and references therein), **generally leading to the negative (positive) phase of the North Atlantic Oscillation (NAO) during EN (LN) years and thus impacting winter temperature and precipitation over Europe (e.g, Ineson and Scaife, 2009)**. These mechanisms are generally grouped into two main pathways, namely the tropospheric and stratospheric pathways (e.g., Bell et al., 2009; Cagnazzo and Manzini, 2009; Ineson and Scaife, 2009; Butler and Polvani, 2011; Butler et al., 2014). Due to a less direct impact and the large internal variability over the North Atlantic, the ENSO teleconnection to the North Atlantic is less robust, and less stationary (Greatbatch, 2004; Deser et al., 2017, 2018; Garfinkel et al., 2019) than that to the North Pacific, with a distinct response in early and late winter (Moron and Gouirand, 2003; Ayarzagüena et al., 2018). In the present study, the tropospheric pathway of the ENSO teleconnection to the North Atlantic is revisited using targeted atmospheric model experiments in order to obtain more robust statistics of this teleconnection and to analyze potential nonlinearities.

ENSO impacts the winter Arctic stratosphere, with a generally weaker (stronger) polar vortex during EN (LN) (e.g., Sassi et al., 2004; García-Herrera et al., 2006; Manzini et al., 2006; Manzini, 2009; Bell et al., 2009; Cagnazzo and Manzini, 2009; Garfinkel and Hartmann, 2008; Iza et al., 2016; Domeisen et al., 2019). While observations and models generally agree on the sign of the winter mean stratospheric response, changes in **the frequency of sudden stratospheric warmings (SSWs)** are less robust (e.g., Butler and Polvani, 2011; Garfinkel et al., 2012; Polvani et al., 2017; Domeisen et al., 2019). **For a summary of the results obtained in these studies see Table 2 in Trascasa-Castro et al. (2019)**. These results are sensitive to the dataset, the time period, and the classification of the SSW events, especially for LN, and hence **time series longer than the current period available for reanalysis data** are necessary in order to make robust conclusions about the ENSO-SSW relationship (Weinberger et al., 2019). **On average, Arctic** stratospheric anomalies can exert a downward impact on the troposphere (Kidston et al., 2015, and references therein), especially over the Arctic and in the North Atlantic **region** (Baldwin and Dunkerton, 2001). A weaker (stronger) stratospheric polar vortex tends to be associated with a negative (positive) phase of the North Atlantic Oscillation (NAO), which impacts temperature and precipitation anomalies **in the North Atlantic region** (Baldwin and Dunkerton, 2001; Ineson and Scaife, 2009; Cagnazzo and Manzini, 2009). Recently, using different atmospheric models Rao and Ren (2016a, b) and Trascasa-Castro et al. (2019) have identified nonlinearities in the stratospheric and North Atlantic response to ENSO, while (Weinberger et al., 2019) find a linear stratospheric response.

The tropospheric pathway of the ENSO teleconnection to the North Atlantic involves different mechanisms. In this study, we focus on the North Pacific downstream effect. **An additional tropospheric** pathway through the tropical Atlantic has been proposed (e.g., Sung et al., 2013; Rodríguez-Fonseca et al., 2016), which might be particularly relevant for strong EN events (Toniazzo and Scaife, 2006; Bell et al., 2009; Hardiman et al., 2019). In the troposphere, quasi-stationary (QS) waves and transient eddies propagate eastward from the North Pacific to the North Atlantic, influencing the circulation in the North Atlantic sector (e.g., Weare, 2010; Li and Lau, 2012a, b; Drouard et al., 2013, 2015; Jiménez-Esteve and Domeisen, 2018; Schemm et al., 2018). **This downstream effect from the North Pacific can be divided into the following mechanisms:**

60 **First**, a direct increase (decrease) in the downstream propagation of transient eddies across North America during EN (LN) conditions generally leads to negative (positive) SLP anomalies in the southern lobe of the NAO (Li and Lau, 2012a, b) that is associated with a southward (northward) shift of the North Atlantic **tropospheric eddy-driven jet**. **A second mechanism acts** through remote baroclinicity changes over North America and the west North Atlantic associated with the PNA phase, which can influence the North Atlantic circulation (Pinto et al., 2011). Such changes in baroclinicity and the background flow affect
65 the genesis of extratropical cyclones over the Rocky mountains, Greenland, and the Gulf stream region (Schemm et al., 2018). **Third**, Drouard et al. (2013, 2015) highlight the role of the meridional tilt of the transient eddies propagating along the jet stream, affecting the type of wave breaking in the North Atlantic during different ENSO phases. Finally, large-scale QS waves also flux energy eastward, which is important for linking the low frequency AL variability with the Icelandic low variability (Honda and Nakamura, 2001; Honda et al., 2005; Orsolini et al., 2008), although this link shows strong decadal variability (e.g.,
70 Honda and Nakamura, 2001; Sun and Tan, 2013). Jiménez-Esteve and Domeisen (2018) show that the eastward propagation of large-scale (zonal wavenumbers 1-3) QS waves generally increases (decreases) during LN (EN) and/or during strong (weak) vortex events.

In summary, the described mechanisms constituting the tropospheric pathway of ENSO through the North Pacific are: changes in the total eastward wave activity fluxes of transient and QS waves, remote changes of baroclinicity and cyclogenesis,
75 and changes in the frequency of the type of wave breaking in the North Atlantic. These mechanisms are not independent and are related for example through the PNA phase. Therefore, **the tropospheric pathway for the ENSO impact on the North Atlantic is driven by** a combination of the previous effects modulated through the **North Pacific** variability. **Here, we focus on the effect of the changes in the total eastward wave activity fluxes (WAF) of transient and QS waves, and the baroclinicity mechanism. We find that nonlinearities in the North Atlantic response to ENSO are better explained in terms of the**
80 **WAF mechanism.**

The stratospheric and tropospheric pathways are also not independent and therefore their respective impacts in the North Atlantic cannot be clearly separated using reanalysis datasets due to the small sample size when subdividing ENSO events into different polar stratosphere states (e.g., Polvani et al., 2017; Jiménez-Esteve and Domeisen, 2018). **Garfinkel et al. (2012) find that ENSO only accounts for some 10% of vortex variability, and that the correlation between Nino3.4 and seasonal mean vortex strength is ~ 0.3 in reanalysis as well as in a range of models. This is supported by Polvani et al. (2017), who report** that approximately 90% of all SSWs are not directly caused by ENSO, and anomalous polar vortex states can occur in either phase of ENSO due to the large internal variability of the polar stratosphere. Also, despite both EN and SSW projecting onto a negative NAO, the surface impacts are not exactly the same (Oehrlein et al., 2019) and they should be considered independently. **To resolve the question of the relative importance of the stratospheric and tropospheric pathways, Bell et al. (2009) compared model simulations with a degraded and not degraded stratosphere and found a distinct and less zonal surface response for a strong EN forcing when the stratospheric pathway is strongly suppressed. In agreement with this finding, Cagnazzo and Manzini (2009) found that low-top models cannot fully reproduce the stratospheric pathway due to their inability to reproduce the SSW increase during EN and therefore the full response in the NAE sector.** Here we **extend the results of the previous studies, and** use idealized atmospheric model experiments forced with

95 ENSO-like SST forcing as in Jiménez-Esteve and Domeisen (2019), while keeping stratospheric winds nudged towards the model climatology. By doing so we are able to remove the stratospheric variability and isolate the tropospheric pathway of ENSO to the North Atlantic, while allowing us to quantify the linearity of this pathway to the North Atlantic.

The paper is organized as follows: A description of the model simulations and the diagnostics employed is provided in section 2. In section 3, we describe the tropospheric pathway of ENSO to the North Atlantic by using experiments where the stratospheric winds are nudged towards climatology. Section 4 explores the spatial structure **as well as the statistical robustness** of the asymmetry and nonlinearity, while Section 5 focuses on the quantification of the nonlinearity as well as the relationship between the North Pacific and the North Atlantic circulation response to ENSO forcing. Finally, the propagation of waves in the troposphere from the North Pacific to the North Atlantic and **how this mechanism contributes** to the model NAO signal is shown in section 6. We close in section 7 with a brief summary and discussion of the main results.

105 2 Data and methods

2.1 Model description and experiments

In this study we use the Isca modelling framework (Vallis et al., 2018), which consists of the Geophysical Fluid Dynamics Laboratory (GFDL) dynamical core coupled with several configurable simplified physical parametrizations, including moist and radiative processes. Isca has been used to simulate atmospheric teleconnections by using SST forcing (e.g., Thomson and Vallis, 2018a, b; Jiménez-Esteve and Domeisen, 2019). In this study we use the same model configuration as in Jiménez-Esteve and Domeisen (2019), see the supplementary information therein for details about the model configuration. In the model, moist and radiative processes are considered through evaporation from the surface and fast condensation (i.e. no explicit liquid water content in the atmosphere), which interacts with the radiation and the convection scheme. We use the multi-band radiation scheme (rrtm) (Mlawer et al., 1997) used in the MiMA model (Jucker and Gerber, 2017), which allows configurable levels of ozone and CO₂ concentrations. We also use realistic topography and the continental outline from the ECMWF model (Dee et al., 2011). The land-sea contrast is achieved by changing surface characteristics such as the mixed layer depth, evaporative resistance and albedo as in Thomson and Vallis (2018a). **SSTs are prescribed and thus we do not use a slab ocean or q-fluxes as in Thomson and Vallis (2018a, b).** The model uses a Gaussian grid with a resolution of T42 and 50 vertical levels up to 0.02 hPa, of which 25 lie above 200 hPa.

120 The model sensitivity experiments consist of a climatological run and four experiments **forced by linearly spaced** magnitudes of tropical ENSO-like SSTs, i.e. strong and moderate EN and LN. In all experiments SSTs are globally prescribed and follow a repeating seasonal cycle (**Figure 1b**). In the climatological run global SSTs follow the 1958-2016 monthly SST climatology from NOAA ERSSTv4 (Huang et al., 2015) (daily values are linearly interpolated). The sensitivity experiments mimic **canonical** tropical Pacific ENSO-like SST anomalies, which consist of four identical spatial patterns (**Figure 1a**) with the same seasonal evolution but with a linearly changing magnitude between moderate and strong ENSO forcing of both signs (**Figure 1b**).

In the four ENSO experiments, climatological SSTs are prescribed north and south of 15 degrees and outside of the Pacific basin [150°E, 280°E] **and only the positive (negative) parts of the SST anomalies are forced for EN (LN)**. Figure 1a displays the December-January-February (DJF) mean SST anomalies for the strong EN forcing, and the three other forcings are multiples of it, with Niño3.4 region SST anomalies peaking slightly above $\pm 1.5(3.0)$ K in November-December-January (NDJ) for moderate (strong) ENSO forcings (Figure 1b). This experiment design, despite **being idealized, allows us to study the nonlinearity/asymmetry in the atmospheric response arising solely due to changes in the ENSO magnitude, while removing the effect of the longitudinal location (central versus eastern Pacific ENSO events) and the asymmetry in the observed ENSO SST anomalies (EN events tend to be stronger than LN events)**.

With the objective to isolate the tropospheric from the stratospheric pathway, the five experiments use the same SST forcing as in Jiménez-Esteve and Domeisen (2019) (i.e. climatological, moderate/strong EN/LN), but the zonal mean winds in the stratosphere are relaxed towards the zonal mean seasonal cycle of the climatological SST simulation (Figure 1c shows the distribution averaged over Dec - Feb). This is achieved by applying a relaxation term of the form $(\bar{U} - \bar{U}_{clim})/\tau$ to the prognostic equation for the zonal wind U at all grid points, where \bar{U} is the zonal mean of U at a given time and \bar{U}_{clim} is the zonal mean climatology target state (Figure 1c). $\tau = \tau(y, p, t)$ is the relaxation time given in days, which varies with pressure p , latitude y , and the month of the year t as

$$\tau(y, p, t) = \begin{cases} \infty & \text{if } p > 0.5p_{trop} \\ 5 + 15.83 \cdot (p/p_{trop} - 0.5) \text{ days} & \text{if } 0.5p_{trop} \leq p \leq 0.2p_{trop} \\ 0.25 \text{ days} & \text{if } p < 0.2p_{trop} \end{cases} \quad (1)$$

where the tropopause pressure $p_{trop}(y, t)$ is computed for each latitude and month of the temperature climatology of the climatological simulation following the World Meteorological Organization definition (Słownik, 1992). Below $0.2p_{trop}$ the relaxation time is 0.25 days, and at pressures higher than $0.5p_{trop}$ the zonal winds evolve freely. Between $0.5p_{trop}$ and $0.2p_{trop}$ a linear function in pressure is applied in order to obtain a smooth transition between the nudged and the freely evolving atmosphere. The relaxation time distribution is shown in Figure 1d. We restrict the nudging to pressure levels above 0.5 times the tropopause level to avoid nudging winds within the upper part of the tropospheric jet, although no significant changes were observed when testing the sensitivity of the results to the position of the nudging zone. However, if the nudging is applied too close to the tropospheric jet, the variability in the troposphere strongly decreases and the response to the tropical ENSO forcing is damped.

In the nudged simulations employed in the present study, the interannual winter (DJF) NAO variance decreases by 40% with respect to the 5 identical simulations when the nudging is not applied, pointing to the important role of the stratosphere in North Atlantic variability. In the North Pacific, the effect of the nudging is much weaker than in the North Atlantic, and the Aleutian low variance decreases only by 10% when the nudging is applied. Additionally, the applied stratospheric nudging does not lead to any significant circulation anomalies in the tropospheric mean flow and the main modes of variability (EOF based) in the North Atlantic remain unaltered (Figure S3). In contrast, when we tested nudging the full climatological wind field instead of the zonal mean component this led to an undesired impact on the tropospheric variability and mean state, probably due to unrealistic changes in the planetary wave propagation.

160 All simulations are initialized from the same spun-up initial conditions, and are integrated for 80 years applying the strato-
spheric nudging described above. An extra spin-up year is removed from the model data for each ENSO SST forcing simulation,
which yields a total of 79 years for each ENSO SST forcing, and 80 years for the climatological SST simulation.

Unless indicated, the statistical significance of the EN and LN responses (forced minus climatological run) is assessed using
a Monte Carlo approach using 1000 random DJF mean combinations of the climatological and forced simulations.

165 2.2 Dynamical diagnostics

2.2.1 Wave Activity Flux for Stationary Waves

The 3D WAF developed by Plumb (1985) is used here to describe the horizontal quasi-stationary (QS) Rossby wave energy
propagation. This flux is phase-independent and parallel to the group velocity of the waves in the almost plane wave approxi-
mation. The horizontal components (F_x, F_y) are computed as follows:

$$170 \begin{pmatrix} F_x \\ F_y \end{pmatrix} = p \cos\phi \begin{pmatrix} \frac{1}{2a^2 \cos^2\phi} \left[\left(\frac{\partial\psi^*}{\partial\lambda} \right)^2 - \psi^* \frac{\partial^2\psi^*}{\partial\lambda^2} \right] \\ \frac{1}{2a^2 \cos\phi} \left(\frac{\partial\psi^*}{\partial\lambda} \frac{\partial\psi^*}{\partial\phi} - \psi^* \frac{\partial^2\psi^*}{\partial\lambda\partial\phi} \right) \end{pmatrix} \quad (2)$$

where a is the Earth's radius, λ is longitude, ϕ is latitude, p is the pressure level divided by $1000hPa$, and ψ is the quasi-
geostrophic stream function, calculated from the geopotential Φ using $\psi = \Phi/2\Omega\sin\phi$, where Ω is the Earth's angular velocity.
Asterisks indicate departures from the zonal mean.

To retain only the contribution from quasi-stationary (QS) waves, the daily means of the geopotential field are low-pass fil-
175 tered with a cutoff period of 10 days **prior** to the calculation of the WAF. We only retain the contribution of zonal wavenumbers
1 to 3, since the large-scale planetary waves exhibit a stronger ENSO sensitivity (Jiménez-Esteve and Domeisen, 2018).

2.2.2 Wave Activity Flux for Transient Eddies

An equivalent WAF based on time deviations of the mean flow and independent of the phase speed allows the tracking of
transient waves ($c \neq 0$) (Plumb, 1986). This formulation is independent of the phase speed, in contrast to the formulations of
180 WAF for transient eddies developed by Takaya and Nakamura (1997, 2001), where the phase speed of the waves has to be
inferred a priori. For a detailed formulation of the transient WAF and its climatology see Plumb (1986) and Nakamura et al.
(2010, 2011). Atmospheric variables are decomposed into the transient part, denoted by $'$ and band-pass filtered with a period
of 2 to 8 days, and its background flow mean part (computed using a 30 days low-pass filter), denoted by an overbar. The
horizontal components of total transient WAF (M_x, M_y) are computed as follows:

$$185 \begin{pmatrix} M_x \\ M_y \end{pmatrix} = \frac{p \cos\phi}{a|\nabla_h \bar{q}|} \begin{pmatrix} \frac{\partial \bar{q}}{\cos\phi \partial \lambda} \overline{u'v'} + \frac{\partial \bar{q}}{\partial \phi} (\overline{v'^2} - \epsilon) \\ \frac{\partial \bar{q}}{\cos\phi \partial \lambda} (\epsilon - \overline{u'^2}) - \frac{\partial \bar{q}}{\partial \phi} \overline{u'v'} \end{pmatrix} + \begin{pmatrix} \bar{u} \\ \bar{v} \end{pmatrix} M \quad (3)$$

where $M = \frac{1}{2}p\cos\phi q'|\nabla_h \bar{q}|$ is the quasi-geostrophic transient wave activity or pseudomomentum, and q is the quasi-geostrophic potential vorticity. The first term on the right hand side in equation 3 is the so-called radiative part of the flux, where

$$\epsilon = \frac{1}{2} \left(\overline{u'^2} + \overline{v'^2} + \frac{Rp^\kappa}{H} \frac{\overline{\theta'^2}}{d\theta_0/dz} \right) \quad (4)$$

190 is the wave energy density, θ is the potential temperature, R is the gas constant of air, $\kappa = R/c_p = 0.286$, c_p is the specific heat at constant pressure, $H = 7\text{km}$ is the scale height. The parameter θ_0 is the potential temperature averaged at each pressure level between $20^\circ N$ and the pole.

2.2.3 Eady growth rate

The maximum Eady growth rate is calculated to study changes in baroclinicity, a proxy for baroclinic eddy development. It is computed as follows:

$$195 \quad \sigma_E = 0.31 \frac{|f| \left| \frac{\partial u}{\partial z} \right|}{N} \quad (5)$$

(Vallis, 2013) where N is the Brunt-Väisälä frequency ($N^2 = \frac{g}{\theta} \frac{\partial \theta}{\partial z}$), g is the acceleration due to gravity, θ is the potential temperature and f is the Coriolis parameter.

3 Isolating the Tropospheric Pathway of ENSO to the North Atlantic

In this section, we investigate the **winter (DJF mean)** North Atlantic circulation response for the idealized ENSO SST forcings
 200 **by** relaxing the stratospheric zonal mean winds towards climatology. These experiments allow us to remove the ENSO remote influence through the winter polar stratosphere, i.e. the stratospheric pathway. **In the model, the North Atlantic response peaks in mid-winter (December to January) and does not exhibit significant changes in pattern, therefore the intra-seasonal variability of the response is not further investigated.**

Figure 2 shows the DJF mean sea level pressure (SLP) and the 250 hPa geopotential height (Z250) model response for
 205 the 4 different ENSO-like SST forcing simulations. The strongest ENSO response is observed in the North Pacific, where during EN conditions the AL intensifies (negative SLP anomalies) and extends eastwards (Fig2a,b). At upper levels (250hPa) the EN response projects onto the positive PNA phase (Fig2e,f), i.e. the first mode of interannual variability in the North Pacific (Wallace and Gutzler, 1981). Qualitatively the opposite-signed pattern occurs for LN forcing, anomalies project onto the negative PNA phase, however significant **asymmetry** in terms of the strength and position of the North Pacific and North
 210 American anomalies can be identified. For example, the response for strong EN (Figure 2a) is **stronger and covers a larger area than** the opposite signed response for strong LN (Figure 2d and **5b**). In this study, we focus on analyzing the response over the North Atlantic sector. The reader is referred to Jiménez-Estevé and Domeisen (2019) for a study of the nonlinearity in the North Pacific region using the same model setup.

In the North Atlantic, the model **generally** reproduces the observed ENSO-North Atlantic teleconnection (e.g., Jiménez-
 215 Estevé and Domeisen, 2018) and projects onto a negative NAO pattern (a decrease in the north-south SLP gradient) for the

strong EN forcing (Figure 2a), whereas **the moderate EN forcing only leads to a significant response in the Northern lobe of the NAO, i.e. the Icelandic low, while having an insignificant impact on the Azores high** (Figure 2b). However, note that the negative NAO dipole for strong EN does not extend into Europe, which is dominated by a positive SLP anomaly, **which matches the observed response for the strongest EN event in 1998, which was characterized by the absence a**
220 **SSW (see Figure 2 in Toniazzo and Scaife (2006)). The same SLP anomaly is obtained by Bell et al. (2009) using model experiments with a degraded stratosphere to remove the stratospheric pathway (see their Figure 11). Thus, although the strong EN forcing projects onto a negative NAO in the Atlantic, the impacts over Europe seem to be distinct. In contrast, the obtained SLP response for moderate EN differs from the study of Bell et al. (2009), which strongly resembles the SLP pattern obtained with the strong EN forcing. A likely explanation for this disagreement is the stronger SST forcing used in their**
225 **study (Nino3.4>2K as compared to Nino3.4~1.5 K in this study).** The LN response **generally** exhibits the opposite-signed circulation anomalies, i.e. a deeper Icelandic low (IL), thus projecting onto the positive NAO phase (Figure 2c,d). For all forcings except for the strong EN, the impact over Europe is weak and insignificant, suggesting that the stratospheric pathway is an essential ingredient to fully describe the ENSO impact over Europe (e.g., Domeisen et al., 2015; Bell et al., 2009; Butler et al., 2014; Polvani et al., 2017; Trascasa-Castro et al., 2019; Cagnazzo and Manzini, 2009; Ineson and Scaife, 2009). The
230 extratropical ENSO response exhibits a strong barotropic structure, i.e. Z250 and SLP anomalies exhibit a very weak westward tilt with height.

Thanks to the linearly varying strength of the ENSO SST forcing we can identify nonlinearities in the response. For example, in the model experiments we observe a saturation of the NAO response for LN: The Icelandic low SLP anomalies for moderate and strong LN are similar in strength, even though the forcing in the tropical Pacific SST is doubled in the latter case (Figure
235 2c-d). Another interesting **result** is that, except for the strong EN forcing, the surface response of the southern lobe of the NAO, i.e. the Azores high, is much weaker than the response of the Icelandic low.

We now analyze the associated changes in the tropospheric winds. Figure 3 displays the zonal wind response (shading) as well as the anomaly vectors at 850 hPa and 250 hPa for the four ENSO forcings. Consistent with the SLP and Z250 anomalies, the EN response is characterized by a strengthening and eastward extension of the Pacific jet, both at lower (Figure 3a,b) and
240 upper levels (Figure 3e,f). This strengthening is not linear, i.e. the response is significantly stronger for strong EN than for moderate EN, consistent with the AL nonlinear response (Jiménez-Estève and Domeisen, 2019). The meridional component of the winds is significantly more poleward along the western coast of North America during EN, advecting warm air to higher latitudes. Opposite-signed anomalies are observed for LN forcing, although **weaker than for EN**. Downstream in the North Atlantic, **on average** the jet stream weakens during EN while it **slightly** strengthens during LN, both at upper and lower levels.
245 The Atlantic jet stream also becomes more tilted during EN (Figure 3e,f), while it is more zonal during LN (Figure 3g,h). **Note that the model North Atlantic jet is too zonally oriented as compared to reanalysis.** While near the surface (at 850 hPa) changes **mainly** correspond to a weakening (strengthening) of the zonal winds for EN (LN), at upper levels (250 hPa) the averaged response corresponds to a southward (northward) shift of the jet location, denoted by the north-south anomaly dipole of zonal wind. **This weakening (strengthening) of the low level zonal winds for EN (LN) might be explained by**
250 **a projection on the East Atlantic (EA) pattern (see Figure 11 in Woollings et al. (2010a)).** The more southern location

of the North Atlantic jet during EN has been also shown to be more thermally driven and less eddy driven (Madonna et al., 2019). **Note that internally generated NAO signals have been suggested to exhibit a more barotropic character than the observed ENSO response in the North Atlantic (Mezzina et al., 2020).**

The temperature at 850 hPa and the lower level baroclinicity in terms of the Eady growth rate (see methods) are shown in Figure 4. Overall, temperature anomalies are stronger over land and are consistent with the changes in the 850 hPa wind circulation (Figure 3a-d). Because SSTs outside of the tropical Pacific are kept fixed to climatological conditions for all experiments, temperature anomalies at 850 hPa over the ocean are much weaker as compared to over land, where skin temperatures are not fixed. The strongest 850 hPa temperature response is therefore located over the North American continent. For EN (LN) experiments, this corresponds to higher (lower) than usual temperatures over Canada and lower (higher) temperatures over the Southern US and Mexico. Thus, in general EN tends to weaken the meridional temperature gradient over North America, whereas LN tends to strengthen it. This has an impact on the baroclinic zone east of the Rocky mountains and at the North American Atlantic coast (Schemm et al., 2018), where the strong land-ocean temperature contrast enhances baroclinicity and fuels the storm track.

Over Europe the strong EN forcing leads to warming (figure 4a), which is opposite to what should be expected from a negative NAO, but consistent with the model positive geopotential anomalies over central Europe (Figure 2e) and increased westerlies over Scandinavia (Figure 3a). The only other forcing leading to significant temperature anomalies over Europe is the moderate LN (figure 4c), with a warming over Scandinavia due to strengthening of the westerly winds related to a deeper IL (Figure 2c). Therefore the tropospheric pathway of ENSO exhibits significant asymmetry in the 850 hPa temperature response to ENSO, with a weak warming both for EN and LN.

Over North America, EN related temperature anomalies weaken the baroclinicity from the central US to the Western Atlantic while strengthening the baroclinicity from the eastern Pacific into the Gulf of Mexico (Figure 4e,f). Qualitatively the opposite behaviour is observed for LN, however the magnitude of the Pacific response is much weaker and over North America the strengthening and northward shift of the baroclinicity does not penetrate as far eastward in the North Atlantic as for the strong EN forcing. A stronger (weaker) baroclinic zone along the North American Atlantic coast leads to a stronger (weaker) North Atlantic storm track and therefore a positive (negative) NAO (Hoskins and Valdes, 1990), which is consistent with Figure 2a-d. For example, the weaker baroclinicity during strong EN tends to weaken the climatological Icelandic low, whereas the strengthening of the meridional temperature gradient during LN can be linked to the intensification of the Icelandic low and the associated near surface westerly winds (Figure 3c,d). **Note that the baroclinicity response over North America is mostly symmetric for moderate events (cp. Figures 4f,g), while it is more asymmetric for strong events (cp. Figures 4e,h).**

4 Spatial pattern and statistical robustness of the nonlinear and asymmetric North Atlantic response to ENSO forcing

We now examine the spatial pattern of the nonlinear **and asymmetric** response to the ENSO tropospheric pathway (cp. Jiménez-Esteve and Domeisen (2019)). We focus on SLP DJF averages over the North Atlantic (Figure 5), while the same analysis for

geopotential height at 250 hPa yields comparable results. **We also do not investigate the intra-seasonal variations of the**
285 **nonlinear/asymmetric response as these are not significant in the simulations. First, we compute** the asymmetry, i.e. the
sum of the EN and LN responses, both for strong and moderate events (Figure 5a,b). The atmospheric response is symmetric
if the same but opposite-signed response is found for EN and LN. The asymmetry of moderate events is then doubled to make
it comparable to the strong events.

For moderate events (Figure 5a), the asymmetry pattern denotes a stronger AL/PNA impact for a moderate EN than for
290 moderate LN, and a stronger positive NAO-like pattern for LN (**compare Figure 2b,c**). **In the North Atlantic the wave train**
structure emerging from the Caribbean might be explained in terms of a stronger Rossby wave source (RWS) response
in that area for moderate EN than for moderate LN (Figure S1) together with the asymmetric response of the transient
WAF (section 6). Whereas in the North Pacific the asymmetry pattern is similar for strong and moderate events, in the Atlantic
the asymmetry is quite different, and for strong events (Figure 5b) the asymmetry pattern arises due to a stronger impact on the
295 southern lobe of the NAO for strong EN compared to LN, and the strong LN having an stronger impact on the IL region than
strong EN (**cp. Figure 2a,d**). Positive asymmetries over Europe result as the distinct response for strong EN events (**Figure**
2a), **although the origin of this response is not clear it might be related to the asymmetry in the tropical North Atlantic**
RWS response (Figure S1). **Note that there are also significant differences between the asymmetry pattern in the North**
Atlantic shown in Figure 5a,b in (Jiménez-Esteve and Domeisen, 2019) and Figure 5a,b in this study. For example,
300 **the strongest negative NAO-like asymmetry in (Jiménez-Esteve and Domeisen, 2019) can be explained in terms of an**
asymmetry in the polar vortex response to ENSO in the model.

The nonlinearity within the EN and LN phase is computed by multiplying the response to moderate events by a factor of
two and subtracting it from the strong event response. For an exactly linear response this would yield zero, as a doubling
of the response would be expected in the linear case. However, for EN (Figure 5c) a zonal wave train pattern emerges. This
305 nonlinearity pattern results from the superlinear deepening of the AL for the strong EN forcing in comparison to the moderate
EN forcing, which is also located further eastward (denoted by a dipole structure, see also Jiménez-Esteve and Domeisen
(2019)). In the North Atlantic, the negative SLP anomaly is suggestive of an eastward extension of the NAO-like dipole
(cp. Figure 2a,b), but also **of a Rossby wave train emerging around the Caribbean region that penetrates into Europe for strong**
EN events. This result **is related to** the finding of Hardiman et al. (2019) and Toniazzo and Scaife (2006), who showed that
310 strong EN events exhibit a different response over Europe than moderate EN events, and that this response might be dominated
by the tropospheric pathway **through the Caribbean and assuming a saturation of the stratospheric pathway. However,**
the stratospheric pathway is not represented in our model experiments, and whether this pathway saturates is still
debated as model studies do not agree. Note than in observations the strongest EN events were not accompanied by
SSW events. Within the LN phase (Figure 5d) most of the nonlinearity is concentrated around the Icelandic low (IL) region,
315 which denotes the saturation of the SLP response between the moderate and strong forcings (Figures 2c,d). **At first this**
saturation of the IL response seems inconsistent with the linear increase in baroclinicity between moderate and strong
LN (cp. Figure 4g,h), suggesting that other tropospheric mechanisms must account for the observed nonlinearity. In

section 6 we show that the role of the WAFs may be responsible for this nonlinearity in the Icelandic low region for LN phase.

320 In order to quantify the statistical robustness of the asymmetric and nonlinear SLP response we employ a Monte Carlo technique following Garfinkel et al. (2018); Weinberger et al. (2019); Deser et al. (2018). The method consists in randomly selecting a sub-sample of increasing size from the pair of simulations used to compute the asymmetric or nonlinear component of the SLP response. This calculation is repeated 2000 times for the different randomly selected sub-samples in order to obtain a bootstrapped probability density function (PDF) of the respective variable. Successively
325 increasing the size of the selected sub-samples allows us to answer the question of how many events must be considered before the nonlinearities/asymmetries become statistically detectable at a certain confidence level (in our case 95%) and for a certain region (see Figure 5 and section 5 for the exact definition of these areas).

Figure 6 displays the 95 and 50% confidence intervals of the asymmetry and nonlinearity of the SLP response in the different predefined regions (shown in different colors). For reference, Figure S2 displays the confidence intervals
330 for each of the terms prior to compute the asymmetry and single phase nonlinearity. In Figure 6, when the whiskers, which indicate the 95% confidence interval, do not cross the zero-line the nonlinearity of that specific index becomes statistically detectable for a given number of events. For example the Aleutian low asymmetry between strong ENSO events becomes statistically detectable at 20 events, while 80 events are needed for the asymmetry in the Azores high index (Figure 6b). For reference Figure S2 displays the estimation of the PDFs for each of the terms used to compute
335 the asymmetry and single phase nonlinearity.

A key message from Figure 6 should be that detecting nonlinearities in observations is still not possible, as a large amount of events is needed before these asymmetries/nonlinearities become statistically detectable. For example, to detect the asymmetry in the NAO between moderate EN and LN (Figure 6a and 5a) more than 50 events would be needed, and to detect the linearity within the LN phase (Figure 6d) in the Icelandic low region at least a sample size of
340 50 events is required.

In order to better understand how the ENSO signal reaches the North Atlantic, in the next section we investigate the relationship between the main modes of variability in the North Pacific and the North Atlantic, i.e. the AL and the NAO, respectively, and how ENSO might affect this connection.

5 The tropospheric link between the North Pacific and the North Atlantic variability

345 The relationship between the North Pacific and the North Atlantic atmospheric circulation is investigated using two indices based on SLP: The AL index is defined as the area-weighted average over [35-60N,180-240E] (green box in Figure 7a), and the NAO index is defined as the SLP difference between the **Icelandic low** (red) [50-75N,60-0W] and the **Azores high** (blue) [20-45N,60-0W] boxes (Figure 7b). Using Empirical Orthogonal Functions (EOF) to define the indices leads to similar results, showing that the model captures the main observed interannual variability in the two regions (see **Figure S2 for the NAO pattern using EOF**). We compute December to March monthly mean values for both indices and for each of the simulations.
350

The two indices are standardized with respect to the climatological simulation. We use monthly instead of seasonal anomalies as these better represent the sub-seasonal timescales on which these pressure systems vary, but using seasonal means leads to comparable results.

355 The model monthly SLP anomalies regressed onto the December to March monthly AL and the NAO indices are shown in Figures 7a,b, respectively. As expected from its definition, the AL regression map has its main signal over the North Pacific and corresponds to a strengthening/weakening of the AL climatological pressure system. In the same map, a north-south dipole over North America extending over the North Atlantic is also identified. This suggests that the negative (positive) NAO signature during EN (LN) can be achieved via the AL modulation and downstream influence, **yet its influence does not significantly extend over Europe**. The same conclusion is obtained when regressing the SLP onto the NAO index, in this case, apart from
360 the expected North Atlantic dipole, which also extends into Europe, a monopole corresponding to the AL is also identified. One interesting point here is that the NAO-like SLP dipole obtained when regressing SLP onto the AL index (Figure 7a) does not reach Europe as compared to the SLP regressed onto the NAO index (Figure 7b). This might be an indication that despite the AL having an influence on the NAO phase, other mechanisms like the **stratospheric or the tropical Atlantic pathway** might be needed to extend the ENSO NAO-like response over Europe.

365 The monthly probability density functions (PDFs) for the 5 model experiments using the different SST forcings are displayed in Figures 7c,d. These PDFs clearly show a strong ENSO influence on the AL index (Figure 7c). Color ticks on the x-axis indicate the composite mean anomalies in units of standard deviations. For the AL, there is a clear nonlinear and asymmetric response to the ENSO forcing, with a much stronger response for EN than for LN. The origin of this nonlinearity and asymmetry with respect to the **ENSO SST forcing can be traced back to the tropical nonlinear relationship between the convective upper troposphere divergent wind response and the underlying tropical SST anomalies (e.g. Johnson and Kosaka, 2016). The North Pacific surface circulation then reacts to the divergence in a linear fashion (see Figure 4c in Jiménez-Esteve and Domeisen (2019))**.
370

The ENSO impact projecting onto the NAO pattern via the tropospheric pathway is much weaker than on the ENSO impact on AL, as has already been shown in the previous section. In general, during winter EN (LN) the tropospheric pathway projects
375 onto a negative (positive) NAO-like pattern (Figure 7d). Strong EN forcing tends to produce a stronger response than the opposite-signed LN. Consistent with Figures 2b,c the moderate LN forcing projects more strongly onto the positive NAO than the moderate EN projects onto a negative NAO. **In fact, the moderate EN response closely resembles a blocking pattern (Figure 2b) which projects onto the second most important mode of variability in the model (Figure S3)**. This figure also shows a saturation of the NAO response for LN forcing, with a mean NAO response around -0.4 standard deviations for both
380 moderate and strong LN, that is, although these are separated by a doubling in the SST forcing. A possible explanation for these nonlinearities in the tropospheric pathway is explored in terms of eastward WAFs in section 6.

While the PDF of the AL is overall symmetric, the PDF of the NAO is negatively skewed, i.e. it has a longer tail towards negative NAO values, which is in agreement with observations (e.g., Woollings et al., 2010b; Domeisen et al., 2018). **We find that EN (LN) tends to increase (decrease) the standard deviation of both the AL and the NAO (Figure S4) and that the strong EN forcing acts to decrease the negative skewness of the climatological NAO making its pdf more symmetric,**
385

similar to the AL (Figures 7c,d and S4). Despite this decrease in the negative skewness, there is still a significant increase in the occurrence of extreme negative NAO events during the strong EN forcing. Note that we cannot compare this figure with reanalysis as there have not been a sufficient number of strong ENSO events in the observational record to calculate the corresponding PDF for the NAO.

390 Figure 8 shows the DJF seasonal mean of the NAO in terms of the AL index for the five simulations with a nudged stratosphere. The correlation coefficient between the winter AL and the NAO indices is significant and larger than 0.5, which is much larger than in reanalysis (Figure S5). Actually, the weaker signal in reanalysis might be related to the destructive interference of other sources of variability and the fact that the three strongest EN events were also accompanied by a strong polar vortex. Figure 8 also illustrates how the large internal variability in the extratropics can mask the North
395 Pacific influence on the NAO variability in response to ENSO. For example, positive and negative values of the NAO index occur for any of the ENSO forcings, as also shown in Figure 11 in Trascasa-Castro et al. (2019). Using observations

Despite the large extratropical variability, and the small signal-to-noise ratio, the relationship between the North Pacific and North Atlantic ENSO response seems to be linear to a good approximation, thus it seems that most of the modeled asymmetry between the strong EN and strong LN (Figure 5b) forcing projecting onto the NAO pattern should mainly originate from the
400 asymmetry in the tropical Pacific upper level divergent wind response (see Figure 4a in Jiménez-Esteve and Domeisen (2019)).

6 Wave activity fluxes of transient and quasi-stationary waves in response to ENSO forcing

The connection between the North Pacific and North Atlantic in the troposphere is predominantly driven by the downstream propagation of QS and transient waves (e.g., Li and Lau, 2012a; Jiménez-Esteve and Domeisen, 2018; Schemm et al., 2018). In this section, we analyze the modeled tropospheric circulation anomalies associated with increased eastward propagation of
405 these waves. Due to the model experiment design, our results isolate the tropospheric pathway from stratospheric interaction, which could otherwise exert an influence on the propagation of waves within the troposphere (e.g., Castanheira and Graf, 2003; Sun and Tan, 2013; Gong et al., 2019).

Figure 9 displays SLP and Z250 composites with respect to strong eastward transient and QS WAF monthly anomalies across North America. Details about the calculation of the WAF are provided in the methods section. The monthly mean eastward
410 component of the transient WAF (M_x) at 250hPa is averaged over the area [20-40N,220-300E] (green box in Figure 9a), which is the climatological location where most of the baroclinic transient eddies propagate (Nakamura et al., 2010). Equivalently, the monthly mean eastward component of the large-scale ($k=1-3$) QS WAF is averaged over a more northern location [45-65N,220-300E] (green box in Figure 9e), i.e. the preferred climatological location of the strongest eastward planetary QS WAF. December to March monthly means of the two indices are standardized with respect to the climatological SST simulation. For
415 the composites we choose a 1.5 standard deviation threshold, but using other thresholds leads to qualitatively similar results.

When the eastward transient WAF is increased over the southern US (green box in Figure 9a) the composite mean AL is stronger than climatology and the North Atlantic anomalies project onto a negative NAO. Thus, our model experiments reproduce well the SLP response to increased eastward transient WAF observed in reanalysis (cp. Figure 3 in Jiménez-Esteve

and Domeisen (2018)). At upper levels (Figure 9b) this teleconnection corresponds to a positive PNA-like Rossby wave train, which coincides with a decrease in the eastward large-scale QS WAF.

The sensitivity to the different ENSO SST forcings is shown as probability distribution functions in Figure 9c, while table 1 shows the percentage of the strong positive (above 1.5 standard deviations) and negative (below -1.5 standard deviations) monthly eastward transient and QS WAF events. According to Figure 9c, in the LN simulations the eastward propagation of transient eddies along the southern part of the US is clearly reduced, with very few events above the 1.5 standard deviations threshold, i.e. 0.3% for both the moderate (strong) LN forcing, respectively (Table 1). In contrast, the eastward transient WAF distribution is shifted to positive values for the strong EN forcing, while no sensitivity is observed for the moderate EN forcing. Strong transient WAF events occur on average for 13% of the months for the strong EN forcing.

An increased eastward QS WAF coincides with a weakening of AL and negative Z250/SLP over north-eastern Canada and Greenland, which projects onto the negative PNA phase and the positive NAO phase (Figure 9d,e). This response is strongly barotropic, which supports the fact that the circulation anomalies are indeed forced by QS waves. While for the increased propagation of transient eddies there is a robust decrease of the QS WAF over Canada (Figure 9b), the opposite is not true. During increased eastward QS WAF events, the westward transient WAF anomalies do not penetrate into the southern NAO region (Figure 9d), and thus there is a weaker impact there.

Because the weakening of the AL is more likely to occur during LN winters (Figure 7c), the probability of increasing the eastward QS WAF (favoring a positive NAO) is larger during LN. This is supported by Figure 9f, which shows a positive shift of the PDF to a more eastward QS WAF during LN. Yet, this response is stronger for the moderate LN than for the strong LN forcing. This is confirmed for the extreme QS WAF events, with a 15.5(9)% frequency for the moderate (strong) LN forcings (Table 1). The opposite QS WAF response is observed for EN experiments, however here the response is more linear as the strongest decrease is observed for the strong EN forcing.

Figure 10 shows the NAO index dependence on the transient and the QS eastward WAF indices. For this figure all five simulations with a nudged stratosphere have been used and monthly averages from December to March are used to better represent the low frequency variability of the NAO. The averaged values of the NAO are distributed into 2-dimensional bins of 0.6×0.6 standard deviations with respect to the transient and QS WAF standardized indices. This representation allows us to differentiate between the individual and combined effects of the transient and the QS waves propagating downstream from the North Pacific to the North Atlantic.

Due to the opposite-signed response to EN and LN, transient and QS WAFs exhibit a correlation, i.e. low (high) values of eastward transient WAF tend to simultaneously occur with high (low) values of QS WAF. Therefore, the NAO response to ENSO results from a constructive interference between these two types of waves (upper-left and lower-right corners in Figure 10). Destructive interference between these two mechanisms can occasionally occur (lower-left and upper-right corner), however these events are less frequent. One possible way to interpret the ENSO impact on the NAO is via the changes in 2-dimensional distribution of these two WAF indices. **The 2-dimensional PDFs for each ENSO forcing** are represented by the colored lines in Figure 10. The saturation of the NAO response during LN (Figure 7d) is consistent with the strong LN forcing leading to weaker transient WAF than the moderate LN, which is compensated by the stronger QS WAF response. Figure 7

also explains why the moderate EN forcing projects weakly onto the negative NAO phase, as neither the transient nor the QS
455 WAF distribution is significantly shifted from the climatological values.

7 Summary and Discussion

Idealized atmospheric model experiments with seasonally evolving prescribed SSTs have been conducted to explore the tro-
pospheric pathway of ENSO to the North Atlantic, as well as potential nonlinearities in this pathway. The model configuration
allows us to remove potential nonlinearities arising from the observed asymmetry in the magnitude and location of LN and
460 EN SST patterns, as well as from extratropical SST effects. To isolate the tropospheric from the stratospheric pathway we use
simulations where stratospheric winds are nudged towards the model zonal mean climatology. Our results can be summarized
as follows:

1. Without a stratospheric influence on the troposphere, the North Atlantic atmospheric response to ENSO forcing can be
explained in terms of the upstream influence from the North Pacific. The response to ENSO in the North Atlantic projects
465 onto a negative (positive) NAO during EN (LN). However, only the strong EN forcing reproduces a complete negative
NAO dipole, whereas the other ENSO forcings exhibit a stronger impact on the Icelandic low.
2. The ENSO tropospheric pathway to the North Atlantic exhibits significant nonlinearity **and asymmetry** with respect
to the tropical Pacific SST forcing, both in terms of the location and the strength of the impacts , **although more than
40-50 events are required before these are statistically detectable**. Strong EN forcing has a stronger impact on the
470 NAO than strong LN forcing, but moderate LN forcing has a significant stronger impact than moderate EN forcing. For
LN forcing, there is a saturation of the **positive** NAO response with no further increase in the NAO index even when
doubling the SST forcing (Figure 7d). Such a saturation effect is not observed for El Niño.
3. The Aleutian low and the NAO modes of variability are **significantly** correlated at monthly and seasonal timescales
(Figure 8) through tropospheric dynamics only.
4. Consistent with reanalysis (Jiménez-Esteve and Domeisen, 2018), in the model EN forcing increases (decreases) the
475 eastward wave activity flux (WAF) of transient eddies (large-scale QS waves) across North America. Because these two
types of WAF exhibit an opposite response for EN and LN (Figure 9), in the model the NAO response to ENSO results
from a constructive interference between the impacts of the two WAFs (Figure 10).**The asymmetry in eastward WAF
response for moderate EN and LN (Figure 9) together with larger Rossby wave source anomalies for moderate
480 EN, likely explain the stronger NAO projection of moderate LN than moderate EN forcing (Figures 5a and 6a).**

While this study has focused on isolating the tropospheric pathway of ENSO to the North Atlantic, in the real world the
stratosphere can play an important role in communicating the ENSO signal to the North Atlantic (e.g., Butler et al., 2014;
Domeisen et al., 2015).

In particular, the role of the stratosphere in contributing to nonlinearities is still debated: When asymmetries between EN and LN in the tropical Pacific are removed, the stratospheric response is significantly more asymmetric (Trascasa-Castro et al., 2019) than if forcing asymmetries are not removed (Weinberger et al., 2019) in different atmospheric models, while Rao and Ren (2016a, b) using a model and reanalysis showed a nonlinear and asymmetric stratospheric wind response. In their experiments, Trascasa-Castro et al. (2019) also find that the NAO response to EN is approximately linear and does not saturate with increasing forcing (up to 3.0 K in DJF), whereas for LN this response is weak and asymmetric with respect to the EN response.

Different modeling studies also find differences in the relative importance of the stratospheric and tropospheric pathways for LN. While Hardiman et al. (2019) using an ensemble of seasonal hindcasts find that the stratospheric pathway to the North Atlantic dominates over the tropospheric pathway for strong LN, i.e. a significant strengthening of the polar vortex; Trascasa-Castro et al. (2019) find a very weak stratospheric response for LN in mid-winter, and thus a insignificant NAO response.

Several factors might be able to explain the differences among the above studies: **e.g. differences in the model and simulation setup, the background SSTs on which the ENSO forcing is imposed** (e.g., Xie et al., 2018), the role of the extratropical SST anomalies, the location and pattern of the ENSO SST forcing, the location and intensity of the climatological planetary-scale stationary waves, **and the stratospheric variability of the model. The too zonally oriented North Atlantic jet bias present in many GCMs (Zappa et al., 2013) might also affect the ability of the model to simulate ENSO teleconnections.** Further work will be necessary to assess the model dependence in relation to the ENSO stratospheric pathway. In the present study we find that nonlinearities in the North Atlantic atmospheric response to ENSO can originate within the tropospheric pathway, independently of the stratospheric response to ENSO.

Another important factor that can impact the ENSO teleconnection to the North Atlantic is decadal variability such as the Pacific Decadal Oscillation (PDO) (Rao et al., 2019) and the Atlantic Multidecadal Oscillation (AMO) (Zhang et al., 2019). The ENSO-stratospheric teleconnection has weakened in recent decades (Hu et al., 2017; Domeisen et al., 2019), which the PDO variability alone cannot explain (Rao et al., 2019), but circulation anomalies over Eastern Europe have likely contributed (Garfinkel et al., 2019). The present study characterizes the North Atlantic response to ENSO and its linearity during these periods when the stratospheric pathway is inactive.

Furthermore, the influence of other sources of interannual variability like the Quasi-Biennial Oscillation (QBO) (e.g., Calvo et al., 2009; Garfinkel and Hartmann, 2010; Hansen et al., 2016), the Madden-Julian Oscillation (MJO) (e.g., Hoell et al., 2014) or Tropical Atlantic SST anomalies (e.g., Toniazzo and Scaife, 2006; Sung et al., 2013; Rodríguez-Fonseca et al., 2016) can modulate the ENSO signal to the North Atlantic. These modes of variability are not present in our simplified model and we can therefore exclude their influence. In the model simulations of Hardiman et al. (2019) the strong EN response in early-to-mid winter is characterized by a Rossby wave source in the Caribbean and tropical Atlantic, with linearly varying strength for symmetric EN and LN events. Our strong EN forcing is characterized by a positive SLP response over Europe, which closely resembles the results obtained by Bell et al. (2009) using simulations with a degraded stratosphere and prescribed SSTs. Thus, although the full wave-like pattern obtained by Hardiman et al. (2019) seems to require SST anomalies outside of the tropical

Pacific (Rodríguez-Fonseca et al., 2016), a Caribbean Rossby wave source might be able to explain the different response for
520 strong EN events over Europe in our experiments. This mechanism might be relevant for strong EN events as suggested by
Toniazzo and Scaife (2006) **assuming a saturation of the stratospheric pathway, or during early winter when the North
Pacific pathway and the stratospheric pathway are not yet fully developed** (Ayarzagüena et al., 2018).

The location of the maximum SST anomalies in the tropical Pacific, i.e. the ENSO flavor, can further influence ENSO
teleconnection. The sensitivity to ENSO flavor has been excluded in this study through the design of the model experiments.
525 Using reanalysis and CIMP5 models, Iza and Calvo (2015); Calvo et al. (2017) found a weaker polar vortex during eastern
Pacific EN and no significant anomalies during central Pacific EN. However, despite the weaker impact on the polar vortex,
Graf and Zanchettin (2012) found that the tropospheric pathway is stronger for central Pacific EN events, leading to a stronger
negative NAO impact in the Atlantic and extending its influence further into Europe. These differences can be explained in
terms of the strength and location of the AL, which is itself linked to the intensity and longitudinal location of the convective
530 response in the tropical Pacific (Garfinkel et al., 2018). The variability in the location of the tropical SST forcing can also
contribute to nonlinearity in the extratropical winter teleconnections (e.g., Yu et al., 2012; Frauen et al., 2014). Thus, further
research will help to understand the nonlinearity in the NAO response arising from the location of the Pacific SST forcing.

In summary, our model experiments confirm most of results obtained using reanalysis (Jiménez-Esteve and Domeisen,
2018), while providing further insight into the nonlinearity **and asymmetry** of the tropospheric pathway of ENSO, which
535 might become more relevant for seasonal prediction in the North Atlantic and Europe due to the observed weakening of the
stratospheric pathway in recent decades.

Code and data availability. The ISCA modelling framework was downloaded from the Github repository (<https://github.com/ExeClim/Isca>).
The ERSSTv4 data was downloaded from the NCAR research data archive (<https://rda.ucar.edu/>) and the ERA-Interim reanalysis from the
ECMWF server (<https://apps.ecmwf.int/datasets/data/>).

540 *Author contributions.* Bernat Jiménez-Esteve performed the model simulations, the data analysis and plotting, and wrote the first draft of the
manuscript. Daniela I.V. Domeisen significantly contributed to the interpretation of the results and the writing of the paper.

Competing interests. The authors declare that they have no conflict of interest

Acknowledgements. The authors would like to thank Stephen Thomson and Edwin Gerber for their helpful comments regarding the model
setup. We are also grateful to Blanca Ayarzagüena and Chaim Garfinkel for constructive discussions. Support from the Swiss National
545 Science Foundation through project PPO0P2_170523 is gratefully acknowledged. The authors would like to thank Paloma Trascasa-Castro
and two anonymous reviewers for their time and insightful comments during the review of our manuscript.

References

- Ayarzagüena, B., Ineson, S., Dunstone, N. J., Baldwin, M. P., and Scaife, A. A.: Intraseasonal Effects of El Niño–Southern Oscillation on North Atlantic Climate, *J. Clim.*, 31, 8861–8873, <https://doi.org/10.1175/JCLI-D-18-0097.1>, 2018.
- 550 Baldwin, M. P. and Dunkerton, T. J.: Stratospheric harbingers of anomalous weather regimes., *Science*, 294, 581–4, <https://doi.org/10.1126/science.1063315>, 2001.
- Barnston, A. G. and Livezey, R. E.: Classification, Seasonality and Persistence of Low-Frequency Atmospheric Circulation Patterns, *Mon. Weather Rev.*, 115, 1083–1126, [https://doi.org/10.1175/1520-0493\(1987\)115<1083:CSAPOL>2.0.CO;2](https://doi.org/10.1175/1520-0493(1987)115<1083:CSAPOL>2.0.CO;2), 1987.
- Bell, C. J., Gray, L. J., Charlton-Perez, A. J., Joshi, M. M., and Scaife, A. A.: Stratospheric communication of El Niño teleconnections to European winter, *J. Clim.*, 22, 4083–4096, <https://doi.org/10.1175/2009JCLI2717.1>, 2009.
- 555 Bjercknes, J.: Atmospheric Teleconnections from the Equatorial Pacific, *Monthly Weather Review*, 97, 163–172, [https://doi.org/10.1175/1520-0493\(1969\)097<0163:ATFTEP>2.3.CO;2](https://doi.org/10.1175/1520-0493(1969)097<0163:ATFTEP>2.3.CO;2), 1969.
- Brönnimann, S.: Impact of El Niño–Southern Oscillation on European climate, *Rev. Geophys.*, 45, <https://doi.org/10.1029/2006RG000199>, 2007.
- 560 Butler, A. H. and Polvani, L. M.: El Niño, La Niña, and stratospheric sudden warmings: A reevaluation in light of the observational record, *Geophys. Res. Lett.*, 38, <https://doi.org/10.1029/2011GL048084>, 2011.
- Butler, A. H., Polvani, L. M., and Deser, C.: Separating the stratospheric and tropospheric pathways of El Niño–Southern Oscillation teleconnections, *Environ. Res. Lett.*, 9, 024014, <https://doi.org/10.1088/1748-9326/9/2/024014>, 2014.
- Cagnazzo, C. and Manzini, E.: Impact of the Stratosphere on the Winter Tropospheric Teleconnections between ENSO and the North Atlantic and European Region, *J. Clim.*, 22, 1223–1238, <https://doi.org/10.1175/2008JCLI2549.1>, 2009.
- 565 Calvo, N., Giorgetta, M. A., Garcia-Herrera, R., and Manzini, E.: Nonlinearity of the combined warm ENSO and QBO effects on the Northern Hemisphere polar vortex in MAECHAM5 simulations, *J. Geophys. Res. Atmos.*, 114, D13 109, <https://doi.org/10.1029/2008JD011445>, 2009.
- Calvo, N., Iza, M., Hurwitz, M. M., Manzini, E., Peña-Ortiz, C., Butler, A. H., Cagnazzo, C., Ineson, S., and Garfinkel, C. I.: Northern Hemisphere Stratospheric Pathway of Different El Niño Flavors in Stratosphere-Resolving CMIP5 Models, *J. Clim.*, 30, 4351–4371, <https://doi.org/10.1175/JCLI-D-16-0132.1>, 2017.
- 570 Castanheira, J. M. and Graf, H.: North Pacific–North Atlantic relationships under stratospheric control?, *J. Geophys. Res.*, 108, 4036, <https://doi.org/10.1029/2002JD002754>, 2003.
- Dee, D. P., Uppala, S. M., Simmons, A. J., Berrisford, P., Poli, P., Kobayashi, S., Andrae, U., Balmaseda, M. A., Balsamo, G., Bauer, P., Bechtold, P., Beljaars, A. C., van de Berg, L., Bidlot, J., Bormann, N., Delsol, C., Dragani, R., Fuentes, M., Geer, A. J., Haimberger, L., Healy, S. B., Hersbach, H., Hólm, E. V., Isaksen, I., Kållberg, P., Köhler, M., Matricardi, M., McNally, A. P., Monge-Sanz, B. M., Morcrette, J. J., Park, B. K., Peubey, C., de Rosnay, P., Tavolato, C., Thépaut, J. N., and Vitart, F.: The ERA-Interim reanalysis: Configuration and performance of the data assimilation system, *Q. J. R. Meteorol. Soc.*, 137, 553–597, <https://doi.org/10.1002/qj.828>, 2011.
- 575 Deser, C., Simpson, I. R., McKinnon, K. A., and Phillips, A. S.: The Northern Hemisphere extratropical atmospheric circulation response to ENSO: How well do we know it and how do we evaluate models accordingly?, *J. Clim.*, 30, 5059–5082, <https://doi.org/10.1175/JCLI-D-16-0844.1>, 2017.
- 580 Deser, C., Simpson, I. R., Phillips, A. S., and McKinnon, K. A.: How Well Do We Know ENSO’s Climate Impacts over North America, and How Do We Evaluate Models Accordingly?, *J. Clim.*, 31, 4991–5014, <https://doi.org/10.1175/JCLI-D-17-0783.1>, 2018.

- 585 Diaz, H. F., Hoerling, M. P., and Eischeid, J. K.: ENSO variability, teleconnections and climate change, *Int. J. Climatol.*, 21, 1845–1862, <https://doi.org/10.1002/joc.631>, 2001.
- Domeisen, D. I., Badin, G., and Koszalka, I. M.: How predictable are the Arctic and North Atlantic Oscillations? Exploring the variability and predictability of the Northern Hemisphere, *J. Clim.*, 31, 997–1014, <https://doi.org/10.1175/JCLI-D-17-0226.1>, 2018.
- Domeisen, D. I. V., Butler, A. H., Fröhlich, K., Bittner, M., Müller, W. A., and Baehr, J.: Seasonal predictability over Europe arising from El Niño and stratospheric variability in the MPI-ESM seasonal prediction system, *J. Clim.*, 28, 256–271, <https://doi.org/10.1175/JCLI-D-14-00207.1>, 2015.
- 590 Domeisen, D. I. V., Garfinkel, C. I., and Butler, A. H.: The Teleconnection of El Niño Southern Oscillation to the Stratosphere, *Rev. Geophys.*, pp. 1–43, <https://doi.org/10.1029/2018RG000596>, 2019.
- Drouard, M., Rivière, G., and Arbogast, P.: The North Atlantic Oscillation Response to Large-Scale Atmospheric Anomalies in the North-eastern Pacific, *J. Atmos. Sci.*, 70, 2854–2874, <https://doi.org/10.1175/JAS-D-12-0351.1>, 2013.
- 595 Drouard, M., Rivière, G., and Arbogast, P.: The Link between the North Pacific Climate Variability and the North Atlantic Oscillation via Downstream Propagation of Synoptic Waves, *J. Clim.*, 28, 3957–3976, <https://doi.org/10.1175/JCLI-D-14-00552.1>, 2015.
- Frauen, C., Dommenges, D., Tyrrell, N., Rezny, M., and Wales, S.: Analysis of the nonlinearity of El Niño-Southern Oscillation teleconnections, *J. Clim.*, 27, 6225–6244, <https://doi.org/10.1175/JCLI-D-13-00757.1>, 2014.
- García-Herrera, R., Calvo, N., Garcia, R. R., and Giorgetta, M. A.: Propagation of ENSO temperature signals into the middle atmosphere: A comparison of two general circulation models and ERA-40 reanalysis data, *J. Geophys. Res. Atmos.*, <https://doi.org/10.1029/2005JD006061>, 2006.
- 600 Garfinkel, C. I. and Hartmann, D. L.: Different ENSO teleconnections and their effects on the stratospheric polar vortex, *J. Geophys. Res. Atmos.*, 113, 1–14, <https://doi.org/10.1029/2008JD009920>, 2008.
- Garfinkel, C. I. and Hartmann, D. L.: Influence of the quasi-biennial oscillation on the North Pacific and El Niño teleconnections, *J. Geophys. Res. Atmos.*, 115, D20 116, <https://doi.org/10.1029/2010JD014181>, 2010.
- 605 Garfinkel, C. I., Butler, A. H., Waugh, D. W., Hurwitz, M. M., and Polvani, L. M.: Why might stratospheric sudden warmings occur with similar frequency in El Niño and La Niña winters?, *J. Geophys. Res. Atmos.*, 117, <https://doi.org/10.1029/2012JD017777>, 2012.
- Garfinkel, C. I., Weinberger, I., White, I. P., Oman, L. D., Aquila, V., and Lim, Y.-K.: The salience of nonlinearities in the boreal winter response to ENSO: North Pacific and North America, *Clim. Dyn.*, 0, 1–18, <https://doi.org/10.1007/s00382-018-4386-x>, 2018.
- 610 Garfinkel, C. I., Schwartz, C., Butler, A. H., Domeisen, D. I., Son, S., and White, I. P.: Weakening of the teleconnection from El Niño-Southern Oscillation to the Arctic stratosphere over the past few decades: What can be learned from subseasonal forecast models?, *J. Geophys. Res. Atmos.*, p. 2018JD029961, <https://doi.org/10.1029/2018JD029961>, 2019.
- Gong, H., Wang, L., Chen, W., Wu, R., Zhou, W., Liu, L., Nath, D., and Lan, X.: Diversity of the Wintertime Arctic Oscillation Pattern among CMIP5 Models: Role of the Stratospheric Polar Vortex, *J. Clim.*, 32, 5235–5250, <https://doi.org/10.1175/JCLI-D-18-0603.1>, 2019.
- 615 Graf, H. F. and Zanchettin, D.: Central Pacific El Niño, the "subtropical bridge," and Eurasian climate, *J. Geophys. Res. Atmos.*, 117, <https://doi.org/10.1029/2011JD016493>, 2012.
- Greatbatch, R. J.: Nonstationary impact of ENSO on Euro-Atlantic winter climate, *Geophys. Res. Lett.*, 31, 4–7, <https://doi.org/10.1029/2003GL018542>, 2004.
- Halpert, M. S. and Ropelewski, C. F.: Surface Temperature Patterns Associated with the Southern Oscillation, *J. Clim.*, 5, 577–593, [https://doi.org/10.1175/1520-0442\(1992\)005<0577:STPAWT>2.0.CO;2](https://doi.org/10.1175/1520-0442(1992)005<0577:STPAWT>2.0.CO;2), 1992.
- 620

- Hansen, F., Matthes, K., and Wahl, S.: Tropospheric QBO-ENSO interactions and differences between the atlantic and pacific, *J. Clim.*, 29, 1353–1368, 2016.
- Hardiman, S. C., Dunstone, N. J., Scaife, A. A., Smith, D. M., Ineson, S., Lim, J., and Fereday, D.: The impact of strong El Niño and La Niña events on the North Atlantic, *Geophys. Res. Lett.*, <https://doi.org/10.1029/2018GL081776>, 2019.
- 625 Hoell, A., Barlow, M., Wheeler, M. C., and Funk, C.: Disruptions of El Niño–Southern Oscillation Teleconnections by the Madden–Julian Oscillation, *Geophysical Research Letters*, 41, 998–1004, <https://doi.org/10.1002/2013GL058648>, 2014.
- Honda, M. and Nakamura, H.: Interannual seesaw between the Aleutian and Icelandic lows. Part II: Its significance in the interannual variability over the wintertime Northern Hemisphere, *J. Clim.*, 14, 4512–4529, [https://doi.org/10.1175/1520-0442\(2001\)014<4512:ISBTAA>2.0.CO;2](https://doi.org/10.1175/1520-0442(2001)014<4512:ISBTAA>2.0.CO;2), 2001.
- 630 Honda, M., Kushnir, Y., Nakamura, H., Yamane, S., and Zebiak, S. E.: Formation, mechanisms, and predictability of the Aleutian-Icelandic low seesaw in ensemble AGCM simulations, *J. Clim.*, 18, 1423–1434, <https://doi.org/10.1175/JCLI3353.1>, 2005.
- Horel, J. D. and Wallace, J. M.: Planetary-Scale Atmospheric Phenomena Associated with the Southern Oscillation, *Mon. Weather Rev.*, 109, 813–829, [https://doi.org/10.1175/1520-0493\(1981\)109<0813:PSAPAW>2.0.CO;2](https://doi.org/10.1175/1520-0493(1981)109<0813:PSAPAW>2.0.CO;2), 1981.
- Hoskins, B. J. and Karoly, D. J.: The Steady Linear Response of a Spherical Atmosphere to Thermal and Orographic Forcing, *J. Atmos. Sci.*, 38, 1179–1196, [https://doi.org/10.1175/1520-0469\(1981\)038<1179:TSLROA>2.0.CO;2](https://doi.org/10.1175/1520-0469(1981)038<1179:TSLROA>2.0.CO;2), 1981.
- 635 Hoskins, B. J. and Valdes, P. J.: On the existence of storm-tracks, *J. Atmos. Sci.*, 47, 1854–1864, [https://doi.org/10.1175/1520-0469\(1990\)047<1854:OTEOST>2.0.CO;2](https://doi.org/10.1175/1520-0469(1990)047<1854:OTEOST>2.0.CO;2), 1990.
- Hu, J., Li, T., Xu, H., and Yang, S.: Lessened response of boreal winter stratospheric polar vortex to El Niño in recent decades, *Clim. Dyn.*, 49, 263–278, <https://doi.org/10.1007/s00382-016-3340-z>, <http://link.springer.com/10.1007/s00382-016-3340-z>, 2017.
- 640 Huang, B., Banzon, V. F., Freeman, E., Lawrimore, J., Liu, W., Peterson, T. C., Smith, T. M., Thorne, P. W., Woodruff, S. D., and Zhang, H. M.: Extended reconstructed sea surface temperature version 4 (ERSST.v4). Part I: Upgrades and intercomparisons, *J. Clim.*, 28, 911–930, <https://doi.org/10.1175/JCLI-D-14-00006.1>, 2015.
- Ineson, S. and Scaife, A. A.: The role of the stratosphere in the European climate response to El Niño, *Nat. Geosci.*, 2, 32–36, <https://doi.org/10.1038/ngeo381>, 2009.
- 645 Iza, M. and Calvo, N.: Role of Stratospheric Sudden Warmings on the response to Central Pacific El Niño, *Geophys. Res. Lett.*, 42, 2482–2489, <https://doi.org/10.1002/2014GL062935>, 2015.
- Iza, M., Calvo, N., and Manzini, E.: The stratospheric pathway of La Niña, *J. Clim.*, 29, 8899–8914, <https://doi.org/10.1175/JCLI-D-16-0230.1>, <http://journals.ametsoc.org/doi/10.1175/JCLI-D-16-0230.1> <https://journals.ametsoc.org/doi/pdf/10.1175/JCLI-D-16-0230.1>, 2016.
- 650 Jiménez-Esteve, B. and Domeisen, D. I.: Nonlinearity in the North Pacific atmospheric response to a linear ENSO forcing, *Geophys. Res. Lett.*, pp. 1–11, <https://doi.org/10.1029/2018gl081226>, 2019.
- Jiménez-Esteve, B. and Domeisen, D. I. V.: The Tropospheric Pathway of the ENSO–North Atlantic Teleconnection, *J. Clim.*, 31, 4563–4584, <https://doi.org/10.1175/JCLI-D-17-0716.1>, 2018.
- Johnson, N. C. and Kosaka, Y.: The impact of eastern equatorial Pacific convection on the diversity of boreal winter El Niño teleconnection patterns, *Clim. Dyn.*, 47, 3737–3765, <https://doi.org/10.1007/s00382-016-3039-1>, <http://link.springer.com/10.1007/s00382-016-3039-1>, 2016.
- 655 Jucker, M. and Gerber, E. P.: Untangling the annual cycle of the tropical tropopause layer with an idealized moist model, *J. Clim.*, 30, 7339–7358, <https://doi.org/10.1175/JCLI-D-17-0127.1>, 2017.

- Kidston, J., Scaife, A. A., Hardiman, S. C., Mitchell, D. M., Butchart, N., Baldwin, M. P., and Gray, L. J.: Stratospheric influence on tropospheric jet streams, storm tracks and surface weather, *Nat. Geosci.*, 8, 433–440, <https://doi.org/10.1038/ngeo2424>, 2015.
- Li, Y. and Lau, N. C.: Impact of ENSO on the atmospheric variability over the North Atlantic in late Winter—Role of transient eddies, *J. Clim.*, 25, 320–342, <https://doi.org/10.1175/JCLI-D-11-00037.1>, 2012a.
- Li, Y. and Lau, N. C.: Contributions of downstream eddy development to the teleconnection between ENSO and the atmospheric circulation over the North Atlantic, *J. Clim.*, 25, 4993–5010, <https://doi.org/10.1175/JCLI-D-11-00377.1>, 2012b.
- Liu, Z. and Alexander, M.: Atmospheric bridge, oceanic tunnel, and global climatic teleconnections, *Rev. Geophys.*, 45, RG2005, <https://doi.org/10.1029/2005RG000172>, 2007.
- Madonna, E., Li, C., and Wettstein, J. J.: Suppressed eddy driving during southward excursions of the North Atlantic jet on synoptic to seasonal time scales, *Atmos. Sci. Lett.*, 20, <https://doi.org/10.1002/asl.937>, <https://onlinelibrary.wiley.com/doi/abs/10.1002/asl.937>, 2019.
- Manzini, E.: Atmospheric science: ENSO and the stratosphere, *Nat. Geosci.*, 2, 749–750, <https://doi.org/10.1038/ngeo677>, 2009.
- Manzini, E., Giorgetta, M. A., Esch, M., Kornblueh, L., and Roeckner, E.: The influence of sea surface temperatures on the northern winter stratosphere: Ensemble simulations with the MAECHAM5 model, *J. Clim.*, 19, 3863–3881, <https://doi.org/10.1175/JCLI3826.1>, <http://dx.doi.org/10.1175/JCLI3826.1>, 2006.
- Mezzina, B., García-Serrano, J., Bladé, I., and Kucharski, F.: Dynamics of the ENSO Teleconnection and NAO Variability in the North Atlantic–European Late Winter, *J. Clim.*, 33, 907–923, <https://doi.org/10.1175/JCLI-D-19-0192.1>, 2020.
- Mlawer, E. J., Taubman, S. J., Brown, P. D., Iacono, M. J., and Clough, S. A.: Radiative transfer for inhomogeneous atmospheres: RRTM, a validated correlated-k model for the longwave, *Journal of Geophysical Research: Atmospheres*, 102, 16 663–16 682, 1997.
- Mo, K. C. and Livezey, R. E.: Tropical–Extratropical Geopotential Height Teleconnections during the Northern Hemisphere Winter, *Mon. Weather Rev.*, 114, 2488–2515, [https://doi.org/10.1175/1520-0493\(1986\)114<2488:TEGHTD>2.0.CO;2](https://doi.org/10.1175/1520-0493(1986)114<2488:TEGHTD>2.0.CO;2), 1986.
- Moron, V. and Gouirand, I.: Seasonal modulation of the El Niño–southern oscillation relationship with sea level pressure anomalies over the North Atlantic in October–March 1873–1996, *Int. J. Climatol.*, 23, 143–155, <https://doi.org/10.1002/joc.868>, 2003.
- Nakamura, M., Kadota, M., Yamane, S., Nakamura, M., Kadota, M., and Yamane, S.: Quasigeostrophic Transient Wave Activity Flux: Updated Climatology and Its Role in Polar Vortex Anomalies, *J. Atmos. Sci.*, 67, 3164–3189, <https://doi.org/10.1175/2010JAS3451.1>, 2010.
- Nakamura, M., Kadota, M., and Yamane, S.: Corrigendum, *J. Atmos. Sci.*, 68, 1841–1842, <https://doi.org/10.1175/JAS-D-11-074.1>, 2011.
- Oehrlein, J., Chiodo, G., and Polvani, L. M.: Separating and quantifying the distinct impacts of El Niño and sudden stratospheric warmings on North Atlantic and Eurasian wintertime climate, *Atmos. Sci. Lett.*, 20, e923, <https://doi.org/10.1002/asl.923>, 2019.
- Orsolini, J. Y., Kvamstø, N. G., T. Kindem, I., Honda, M., and Nakamura, H.: Influence of the Aleutian–Icelandic Low Seesaw and ENSO onto the Stratosphere in Ensemble Winter Hindcasts, *J. Meteorol. Soc. Japan*, 86, <https://doi.org/10.2151/jmsj.86.817>, 2008.
- Philander, S. G. H.: *El Niño, La Niña, and the Southern Oscillation*, 1990.
- Pinto, J. G., Reyers, M., and Ulbrich, U.: The variable link between PNA and NAO in observations and in multi-century CGCM simulations, *Clim. Dyn.*, 36, 337–354, <https://doi.org/10.1007/s00382-010-0770-x>, 2011.
- Plumb, R. A.: On the Three-Dimensional Propagation of Stationary Waves, *J. Atmos. Sci.*, 42, 217–229, [https://doi.org/10.1175/1520-0469\(1985\)042<0217:OTTDPO>2.0.CO;2](https://doi.org/10.1175/1520-0469(1985)042<0217:OTTDPO>2.0.CO;2), 1985.
- Plumb, R. A.: Three-Dimensional Propagation of Transient Quasi-Geostrophic Eddies and Its Relationship with the Eddy Forcing of the Time—Mean Flow, *J. Atmos. Sci.*, 43, 1657–1678, [https://doi.org/10.1175/1520-0469\(1986\)043<1657:TDPOTQ>2.0.CO;2](https://doi.org/10.1175/1520-0469(1986)043<1657:TDPOTQ>2.0.CO;2), 1986.

- Polvani, L. M., Sun, L., Butler, A. H., Richter, J. H., and Deser, C.: Distinguishing stratospheric sudden warmings from ENSO as key drivers of wintertime climate variability over the North Atlantic and Eurasia, *J. Clim.*, 30, 1959–1969, <https://doi.org/10.1175/JCLI-D-16-0277.1>, 2017.
- Rao, J. and Ren, R.: Asymmetry and nonlinearity of the influence of ENSO on the northern winter stratosphere: 1. Observations, *J. Geophys. Res. Atmos.*, 121, 9000–9016, <https://doi.org/10.1002/2015JD024520>, <http://doi.wiley.com/10.1002/2015JD024520>, 2016a.
- 700 Rao, J. and Ren, R.: Asymmetry and nonlinearity of the influence of ENSO on the northern winter stratosphere: 2. Model study with WACCM, *J. Geophys. Res. Atmos.*, 121, 9017–9032, <https://doi.org/10.1002/2015JD024521>, <http://doi.wiley.com/10.1002/2015JD024521>, 2016b.
- Rao, J., Garfinkel, C. I., and Ren, R.: Modulation of the Northern Winter Stratospheric El Niño–Southern Oscillation Teleconnection by the PDO, *J. Clim.*, pp. JCLI–D–19–0087.1, <https://doi.org/10.1175/JCLI-D-19-0087.1>, 2019.
- 705 Rodríguez-Fonseca, B., Suárez-Moreno, R., Ayarzagüena, B., López-Parages, J., Gómara, I., Villamayor, J., Mohino, E., Losada, T., and Castaño-Tierno, A.: A review of ENSO influence on the North Atlantic. A non-stationary signal, *Atmosphere (Basel)*, 7, 1–19, <https://doi.org/10.3390/atmos7070087>, 2016.
- Ropelewski, C. F. and Halpert, M. S.: Global and Regional Scale Precipitation Patterns Associated with the El Niño/Southern Oscillation, *Mon. Weather Rev.*, 115, 1606–1626, [https://doi.org/10.1175/1520-0493\(1987\)115<1606:GARSPP>2.0.CO;2](https://doi.org/10.1175/1520-0493(1987)115<1606:GARSPP>2.0.CO;2), 1987.
- 710 Sardeshmukh, P. D. and Hoskins, B. J.: The Generation of Global Rotational Flow by Steady Idealized Tropical Divergence, *J. Atmos. Sci.*, 45, 1228–1251, [https://doi.org/10.1175/1520-0469\(1988\)045<1228:TGOGRF>2.0.CO;2](https://doi.org/10.1175/1520-0469(1988)045<1228:TGOGRF>2.0.CO;2), 1988.
- Sassi, F., Kinnison, D., Boville, B. A., Garcia, R. R., and Roble, R.: Effect of El Niño–Southern Oscillation on the dynamical, thermal, and chemical structure of the middle atmosphere, *J. Geophys. Res. D Atmos.*, 109, D17 108, <https://doi.org/10.1029/2003JD004434>, 2004.
- Schemm, S., Riviére, G., Ciasto, L. M., and Li, C.: Extratropical cyclogenesis changes in connection with tropospheric ENSO teleconnections to the North Atlantic: Role of stationary and transient waves., *J. Atmos. Sci.*, pp. JAS–D–17–0340.1, <https://doi.org/10.1175/JAS-D-17-0340.1>, 2018.
- 715 Seager, R., Naik, N., Ting, M., Cane, M. A., Harnik, N., and Kushnir, Y.: Adjustment of the atmospheric circulation to tropical pacific sst anomalies: Variability of transient eddy propagation in the pacific-north america sector, *Q. J. R. Meteorol. Soc.*, 136, 277–296, <https://doi.org/10.1002/qj.588>, 2010.
- 720 Slowik, W.: International meteorological vocabulary, Tech. rep., WMO/OMM/IMGW, 182, Geneva, 1992.
- Sun, J. and Tan, B.: Mechanism of the wintertime Aleutian Low-Icelandic Low seesaw, *Geophys. Res. Lett.*, 40, 4103–4108, <https://doi.org/10.1002/grl.50770>, 2013.
- Sung, M. K., Ham, Y. G., Kug, J. S., and An, S. I.: An alterative effect by the tropical North Atlantic SST in intraseasonally varying El Niño teleconnection over the North Atlantic, *Tellus, Ser. A Dyn. Meteorol. Oceanogr.*, 65, 1–13, <https://doi.org/10.3402/tellusa.v65i0.19863>, 2013.
- 725 Takaya, K. and Nakamura, H.: A formulation of a wave activity flux for stationary Rossby waves on a zonally varying basic flow, *Geophys Res Lett*, 24, 2985–2988, <https://doi.org/10.1029/97GL03094>, 1997.
- Takaya, K. and Nakamura, H.: A Formulation of a Phase-Independent Wave-Activity Flux for Stationary and Migratory Quasigeostrophic Eddies on a Zonally Varying Basic Flow, *J. Atmos. Sci.*, 58, 608–627, [https://doi.org/10.1175/1520-0469\(2001\)058<0608:AFOAPI>2.0.CO;2](https://doi.org/10.1175/1520-0469(2001)058<0608:AFOAPI>2.0.CO;2), 2001.
- 730 Thomson, S. I. and Vallis, G. K.: Atmospheric Response to SST anomalies. Part 1: Background-state dependence, teleconnections and local effects in winter, *J. Atmos. Sci.*, <https://doi.org/10.1175/JAS-D-17-0297.1>, 2018a.

- Thomson, S. I. and Vallis, G. K.: Atmospheric response to SST anomalies. Part II: Background-state dependence, teleconnections, and local effects in summer, *J. Atmos. Sci.*, 75, 4125–4138, <https://doi.org/10.1175/JAS-D-17-0298.1>, 2018b.
- 735 Toniazzo, T. and Scaife, A. A.: The influence of ENSO on winter North Atlantic climate, *Geophys. Res. Lett.*, 33, <https://doi.org/10.1029/2006GL027881>, 2006.
- Trascasa-Castro, P., Maycock, A. C., Scott Yiu, Y. Y., and Fletcher, J. K.: On the linearity of the stratospheric and Euro-Atlantic sector response to ENSO, *J. Clim.*, pp. JCLI-D-18-0746.1, <https://doi.org/10.1175/JCLI-D-18-0746.1>, 2019.
- Trenberth, K. E., Branstator, G. W., Karoly, D., Kumar, A., Lau, N.-C., and Ropelewski, C.: Progress during TOGA in understanding and modeling global teleconnections associated with tropical sea surface temperatures, *J. Geophys. Res. Ocean.*, 103, 14 291–14 324, <https://doi.org/10.1029/97JC01444>, 1998.
- 740 Vallis, G. K.: *Atmospheric and Oceanic Fluid Dynamics*, Cambridge University Press, 2013.
- Vallis, G. K., Colyer, G., Geen, R., Gerber, E., Jucker, M., Maher, P., Paterson, A., Pietschnig, M., Penn, J., and Thomson, S. I.: Isca, v1.0: A framework for the global modelling of the atmospheres of Earth and other planets at varying levels of complexity, *Geosci. Model Dev.*, 11, 843–859, <https://doi.org/10.5194/gmd-11-843-2018>, 2018.
- 745 Wallace, J. M. and Gutzler, D. S.: Teleconnections in the Geopotential Height Field during the Northern Hemisphere Winter, *Mon. Weather Rev.*, 109, 784–812, [https://doi.org/10.1175/1520-0493\(1981\)109<0784:TITGHF>2.0.CO;2](https://doi.org/10.1175/1520-0493(1981)109<0784:TITGHF>2.0.CO;2), 1981.
- Weare, B. C.: Tropospheric-stratospheric wave propagation during El Niño–Southern Oscillation, *J. Geophys. Res.*, 115, D18 122, <https://doi.org/10.1029/2009JD013647>, 2010.
- 750 Weinberger, I., Garfinkel, C. I., White, I. P., and Oman, L. D.: The salience of nonlinearities in the boreal winter response to ENSO : Arctic stratosphere and Europe, *Clim. Dyn.*, <https://doi.org/10.1007/s00382-019-04805-1>, 2019.
- Woollings, T., Hannachi, A., and Hoskins, B.: Variability of the North Atlantic eddy-driven jet stream, *Q. J. R. Meteorol. Soc.*, 136, 856–868, <https://doi.org/10.1002/qj.625>, <http://doi.wiley.com/10.1002/qj.625>, 2010a.
- Woollings, T., Hannachi, A., Hoskins, B., and Turner, A.: A regime view of the North Atlantic oscillation and its response to anthropogenic forcing, *J. Clim.*, 23, 1291–1307, <https://doi.org/10.1175/2009JCLI3087.1>, 2010b.
- 755 Xie, F., Zhou, X., Li, J., Sun, C., Feng, J., and Ma, X.: The key role of background sea surface temperature over the cold tongue in asymmetric responses of the Arctic stratosphere to El Niño–Southern Oscillation, *Environ. Res. Lett.*, 13, 114 007, <https://doi.org/10.1088/1748-9326/aae79b>, 2018.
- Yu, J.-Y., Zou, Y., Kim, S. T., and Lee, T.: The changing impact of El Niño on US winter temperatures, *Geophys. Res. Lett.*, 39, <https://doi.org/10.1029/2012GL052483>, 2012.
- 760 Zappa, G., Shaffrey, L. C., and Hodges, K. I.: The ability of CMIP5 models to simulate North Atlantic extratropical cyclones, *J. Clim.*, 26, 5379–5396, <https://doi.org/10.1175/JCLI-D-12-00501.1>, <http://journals.ametsoc.org/doi/10.1175/JCLI-D-12-00501.1>, 2013.
- Zhang, T., Perlwitz, J., and Hoerling, M. P.: What is responsible for the strong observed asymmetry in teleconnections between El Niño and La Niña?, *Geophys. Res. Lett.*, 41, 1019–1025, <https://doi.org/10.1002/2013GL058964>, 2014.
- 765 Zhang, W., Wang, Z., Stuecker, M. F., Turner, A. G., Jin, F. F., and Geng, X.: Impact of ENSO longitudinal position on teleconnections to the NAO, *Clim. Dyn.*, 52, 257–274, <https://doi.org/10.1007/s00382-018-4135-1>, <http://link.springer.com/10.1007/s00382-018-4135-1>, 2019.

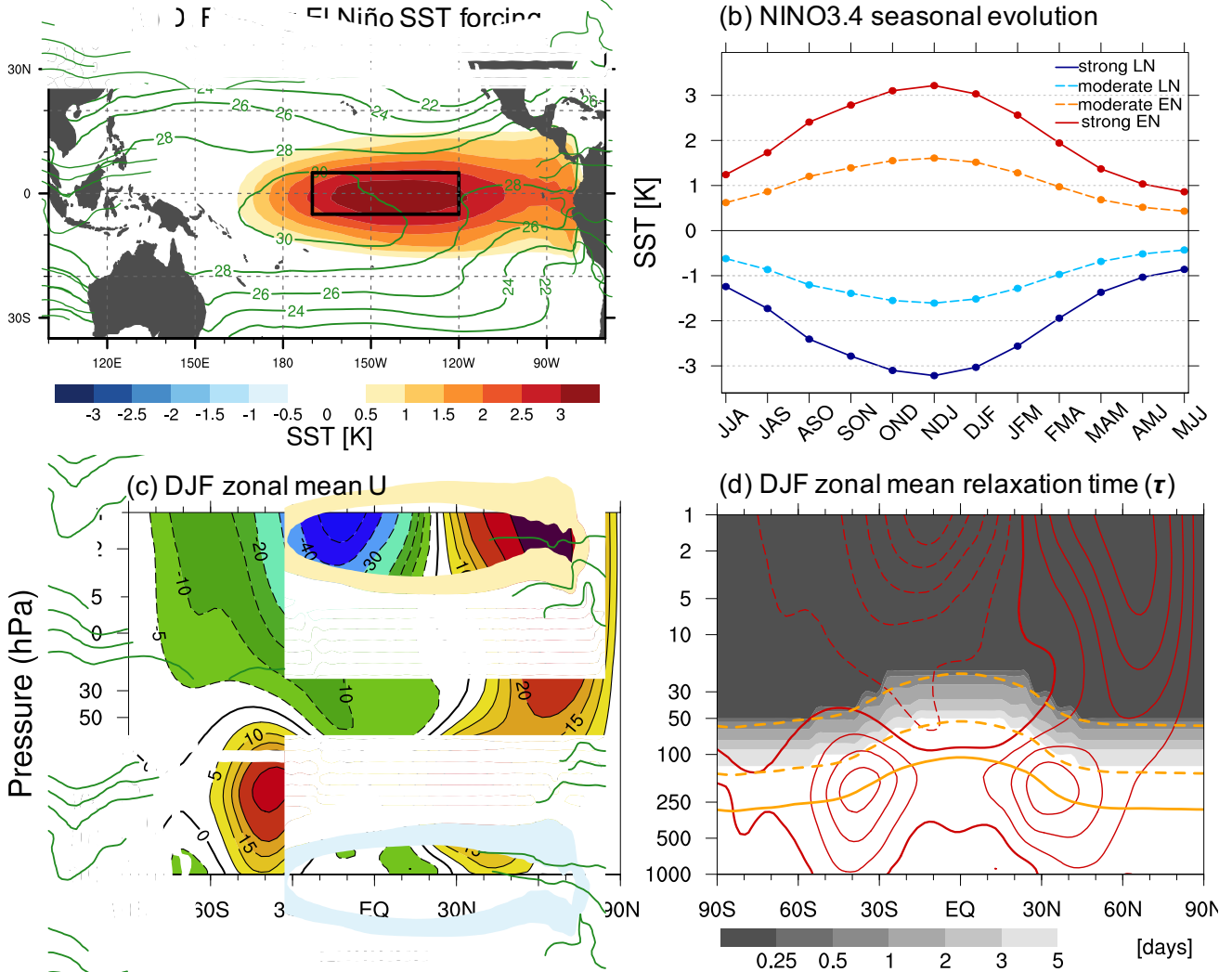


Figure 1. (a) DJF SST anomaly pattern in the tropical Pacific for the strong El Niño forcing simulation. (b) The seasonal evolution of the SST anomalies in the NINO3.4 region (black box in (a)) for the four types of SST ENSO forcings. (c) The DJF zonal mean zonal wind (U) in the climatological SST simulation. (d) The DJF zonal mean relaxation timescale (τ) in days. In (d), red contours represent U as in (c), the solid orange line represents the DJF mean tropopause height and the dashed orange lines represent the $0.5p_{trop}$ and $0.2p_{trop}$ levels, which denote the limits for the transition area of the nudging.

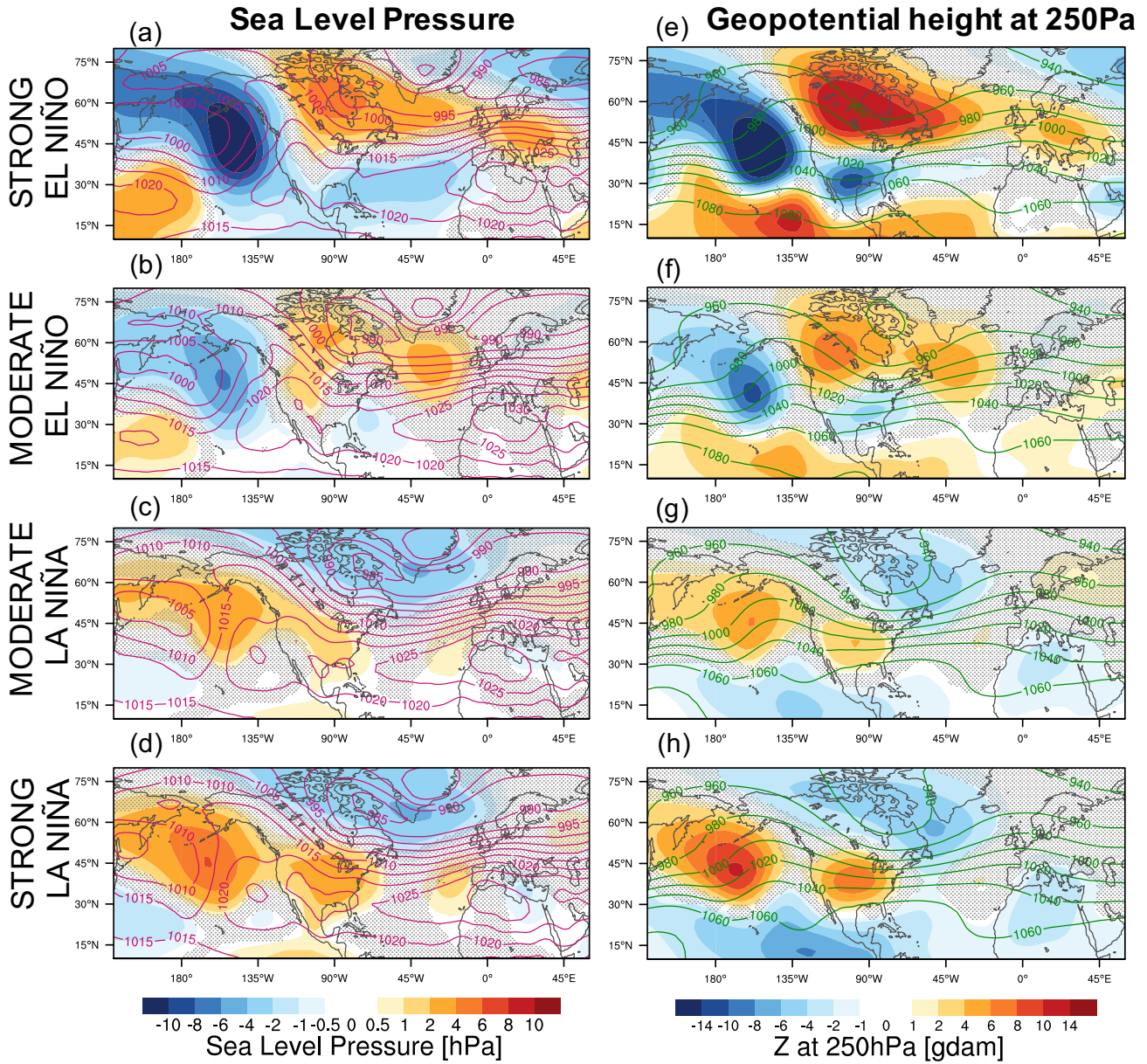


Figure 2. (a-d) DJF SLP and (e-h) DJF mean Z250 model response for the nudged stratosphere simulations with (a,e) strong EN, (b,f) moderate EN, (c,g) moderate LN, and (d,h) strong LN forcing. Contour lines indicate absolute values of SLP (hPa) and Z250 (gdam = geopotential decameters), respectively. Non-statistically significant values below the 95% confidence level are dotted in grey.

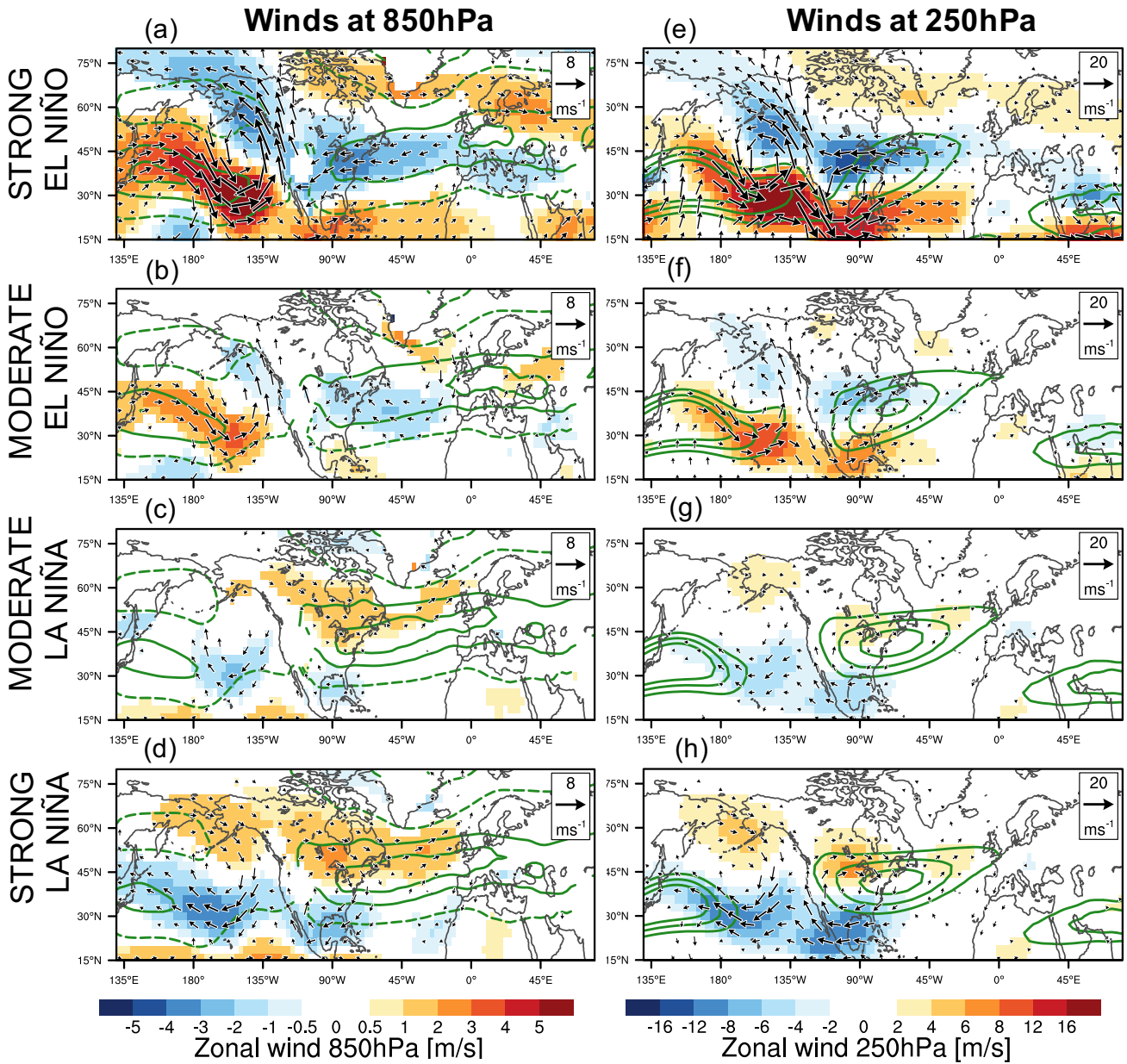


Figure 3. As in Figure 2, but for the zonal wind (a-d) at 850 hPa and (e-h) at 250 hPa. Arrows display the zonal and meridional wind anomalies. Green contour lines show the absolute values of the zonal wind component for each simulation [0 (dashed), 5 and 15 m/s in (a-d) and 30, 40 and 50 m/s in (e-h), respectively]. Only statistically significant values above the 95% level are shown.

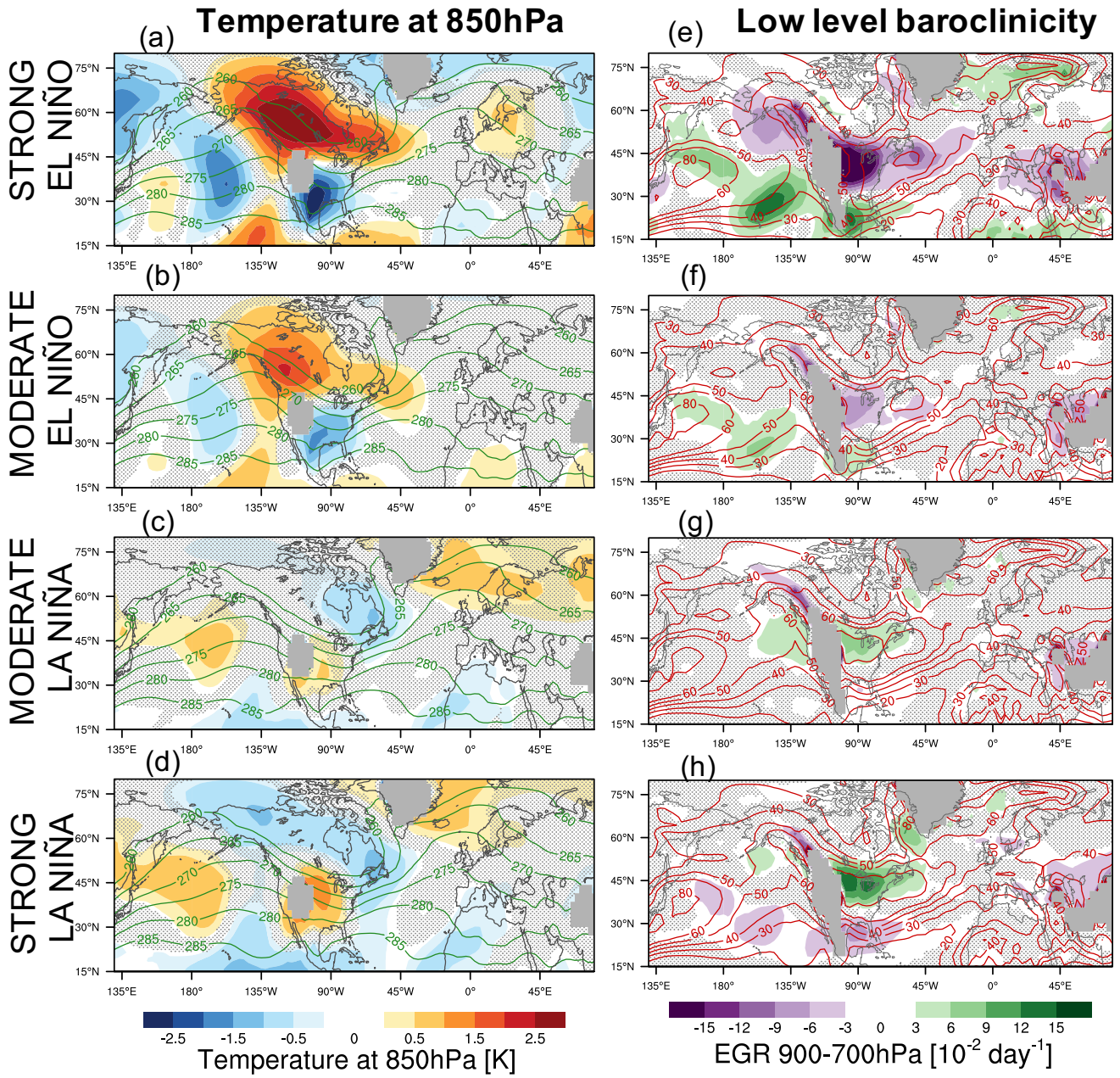


Figure 4. As in Figure 2, but for (a-d) the temperature at 850 hPa and (e-h) the Eady growth rate (EGR) vertically integrated between 900 and 700 hPa. Contour lines indicate the absolute values of temperature (K) and EGR (10^{-2} day^{-1}), respectively. Non-statistically significant values below the 95% confidence level are dotted in grey.

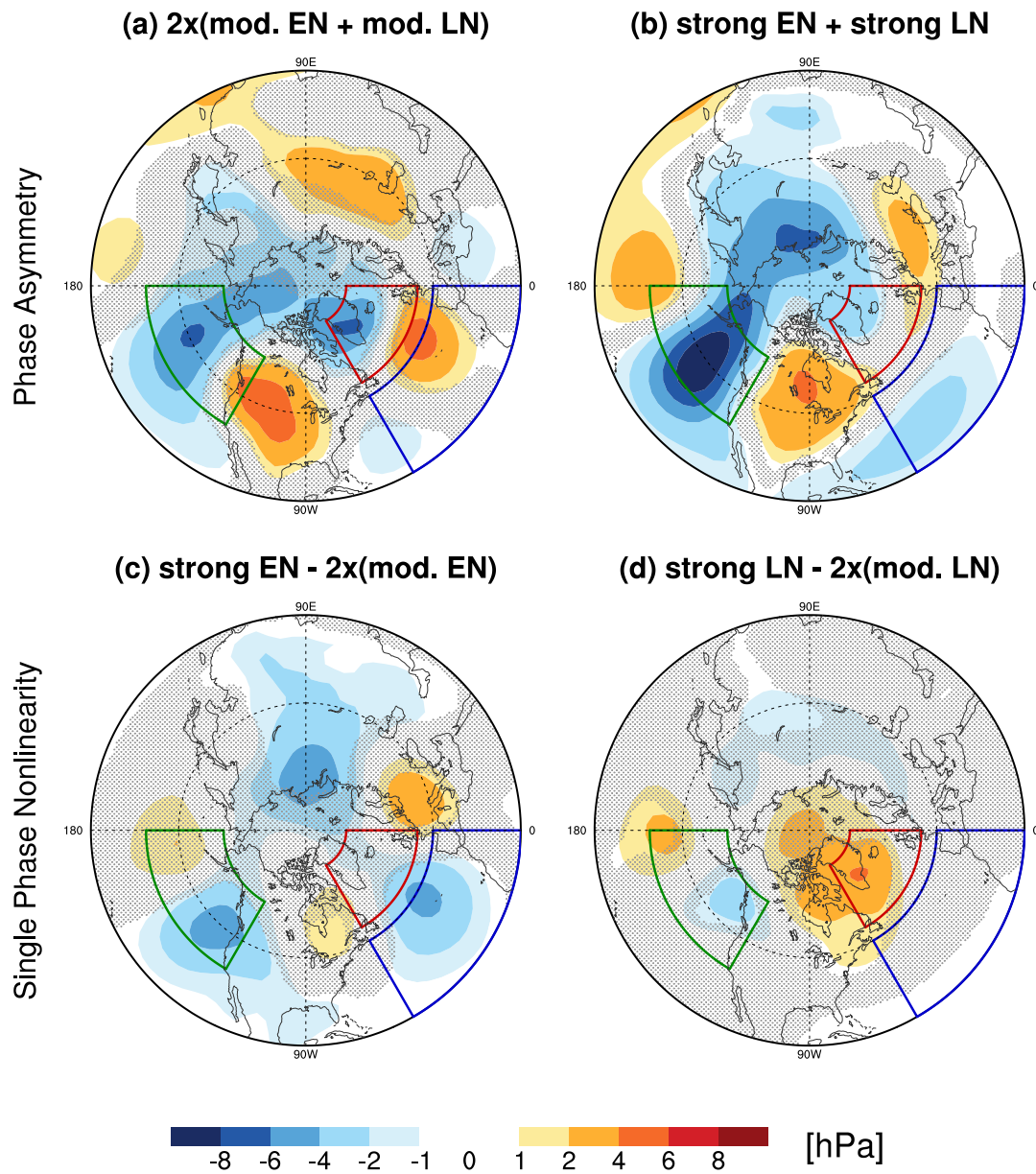


Figure 5. DJF model SLP response asymmetry for (a) twice the moderate and (b) strong ENSO forcings. (c) EN and (d) LN single phase nonlinearity. See the main text for definitions. **Green, red and blue boxes indicate the regions used to define the AL, the Icelandic low and Azores high regions, respectively, see main text for details. The NAO is computed as the difference between the Icelandic low and the Azores high index. Non-statistically significant values below the 95% confidence level are dotted in grey.**

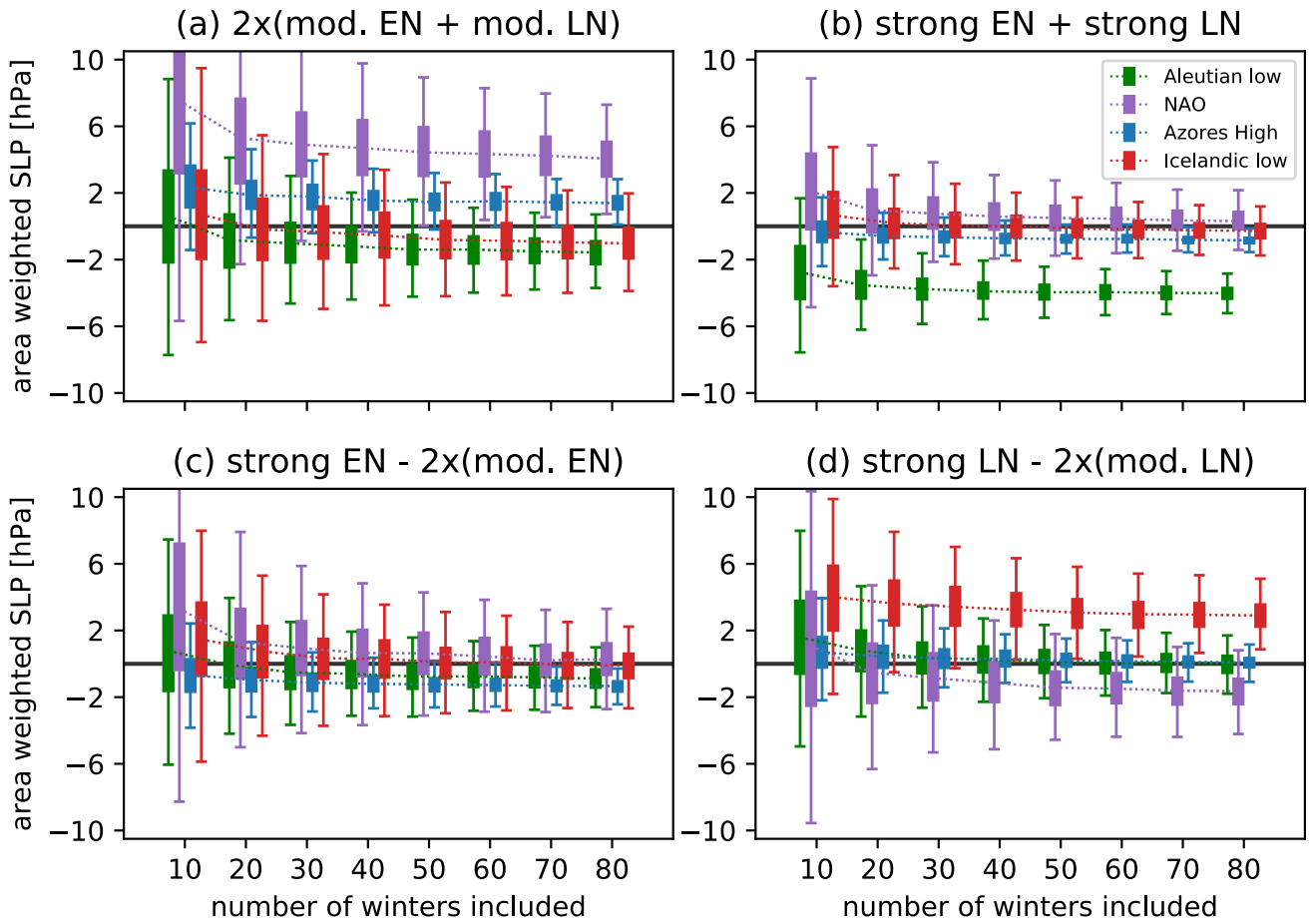


Figure 6. Box plot displaying the 95(50)% confidence intervals indicated by the whiskers (solid boxes) of the DJF model SLP asymmetric response for (a) twice the moderate and (b) strong ENSO forcings when the winter anomalies in these experiments are randomly sub-sampled in groups of increasing size (shown on the x-axis). Colors indicate the different SLP indices (green: Aleutian low, purple: NAO, blue: Azores High, red: Icelandic low). (c) the same as (a,b) but for EN and (d) LN single phase nonlinearity. When the whiskers do not touch the zero-line for a specific sample size and magnitude, then the asymmetry/nonlinearity is statistically detectable at the 95% confidence interval.

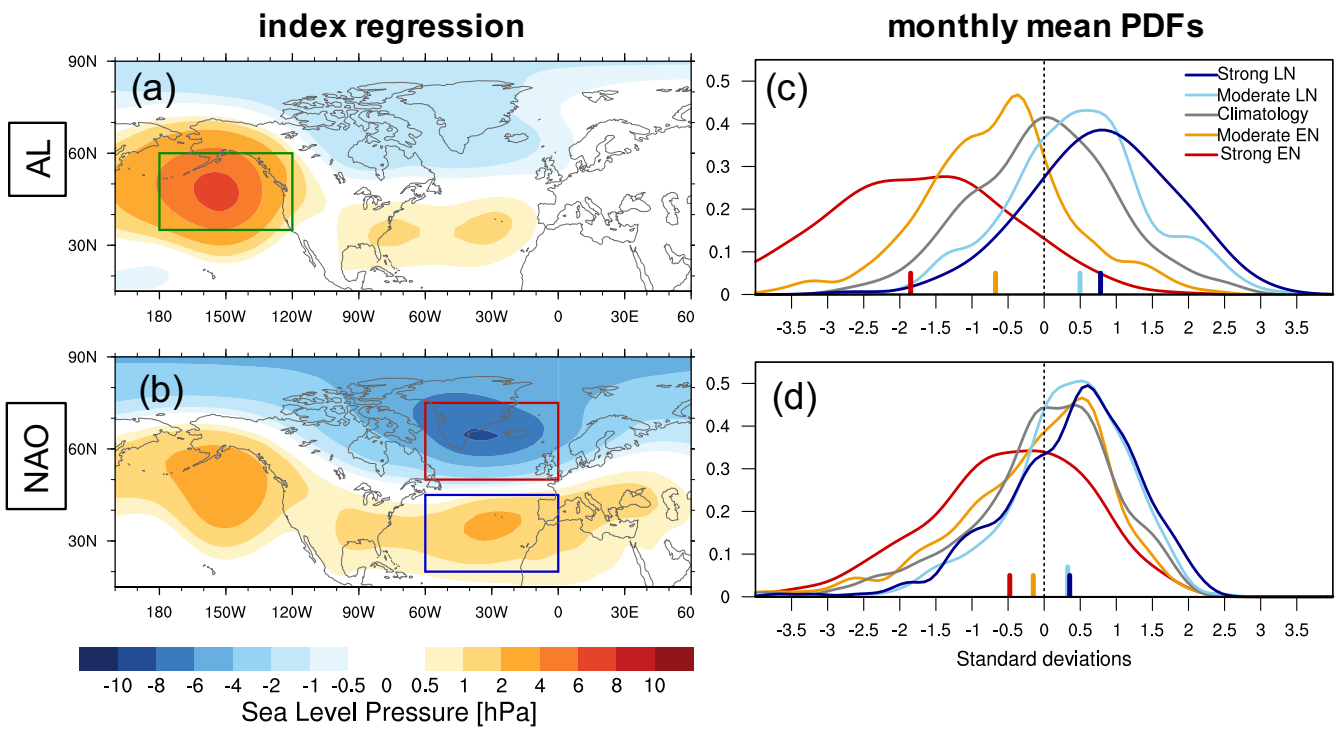


Figure 7. December to March monthly SLP (in hPa) regressed onto (a) the AL and (b) the NAO indices, using the five simulations with stratospheric nudging (396 years). Green, red and blue boxes indicate the regions used to define the AL and NAO indices, respectively, see main text for details. The PDFs of the December-January-February-March standardized monthly means for (c) the AL and (d) the NAO indices. Colors represent the PDFs for the different ENSO forcings (red: strong EN, orange: moderate EN, grey: climatology, light blue: moderate LN, dark blue: strong LN).

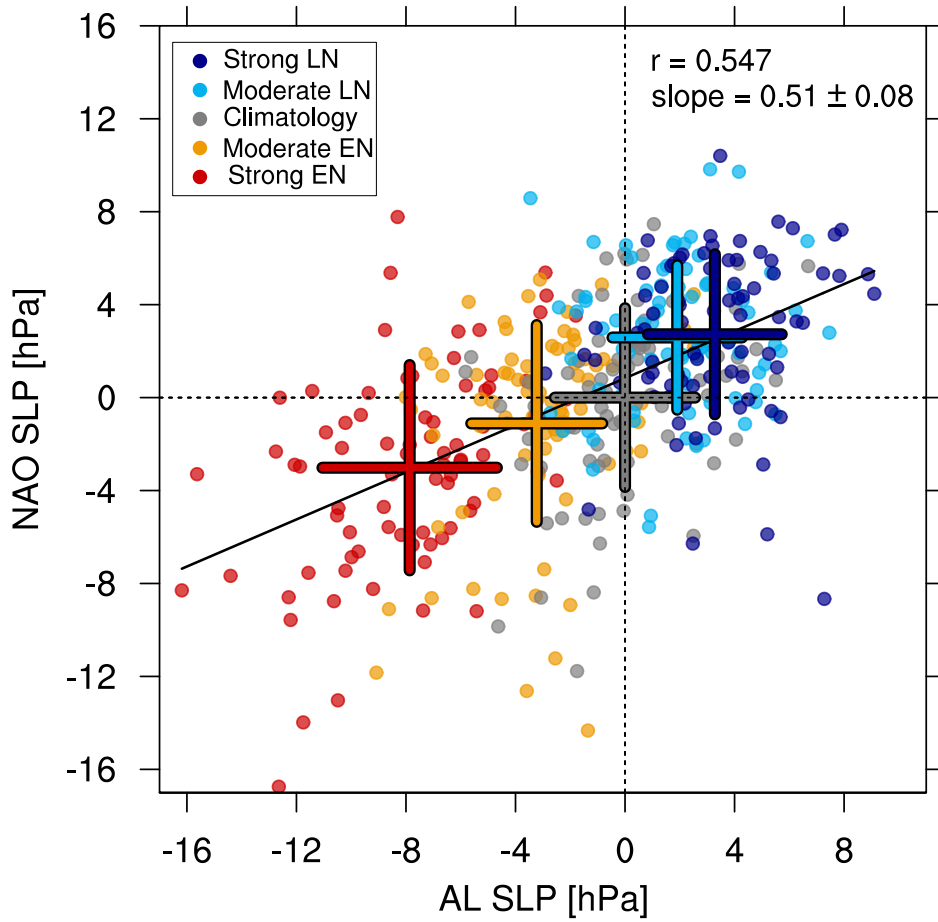


Figure 8. Scatter plot of the DJF mean NAO index versus the DJF mean AL index (not standardized) for all five experiments using nudging in the stratosphere (total of 396 years). Different colors identify the different ENSO forcings (red: strong EN, orange: moderate EN, grey: climatology, light blue: moderate LN, dark blue: strong LN). Crosses are centered at the mean values for each ENSO experiment, with the limits of the vertical and horizontal components corresponding to ± 1 standard deviations of the NAO and AL indices respectively. The correlation coefficient (r) as well as the slope of the linear regression (black line) is shown at the top left corner. The slope error corresponds to a 95% confidence interval assuming a Gaussian distribution.

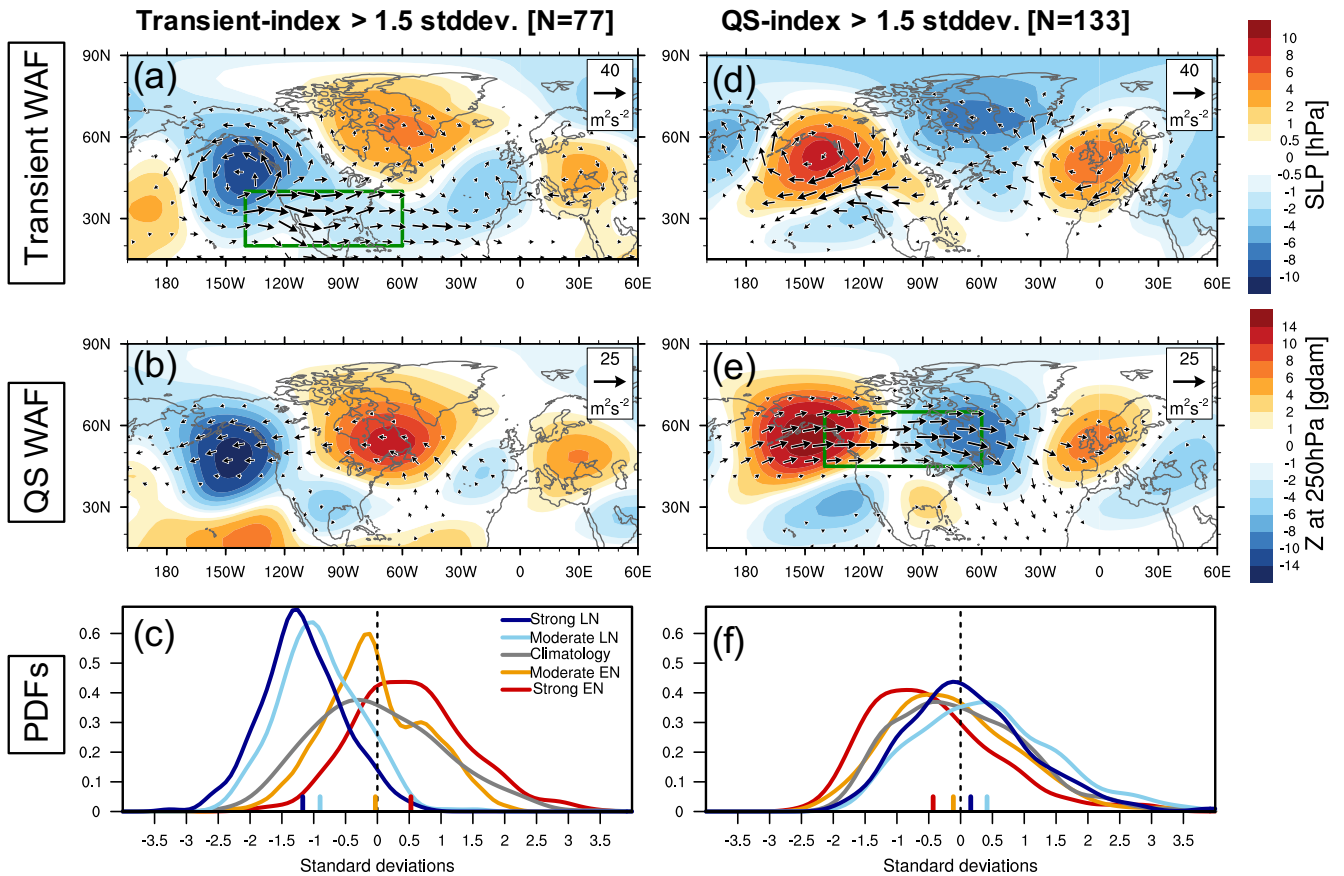


Figure 9. December to March monthly mean anomaly composites of (a,d) SLP (color shading) and transient WAF (arrows), and (b,e) Z250 (shading) and QS WAF (arrows), for months when anomalously strong eastward WAF of (a,b) transient eddies and (d,e) QS ($k=1-3$) waves occur. Events are defined using a threshold of 1.5 standard deviations for each of the indices. At the top, values in brackets indicate the total number of months considered in each composite. Green boxes indicate the regions where the eastward component of the WAF has been averaged for (a) transient and (e) QS waves. The PDF of the December to March standardized monthly means for (c) the M_x -index and (f) the F_x -index. Colors indicate different ENSO forcings (red: strong EN, orange: moderate EN, grey: climatology, light blue: moderate LN, dark blue: strong LN).

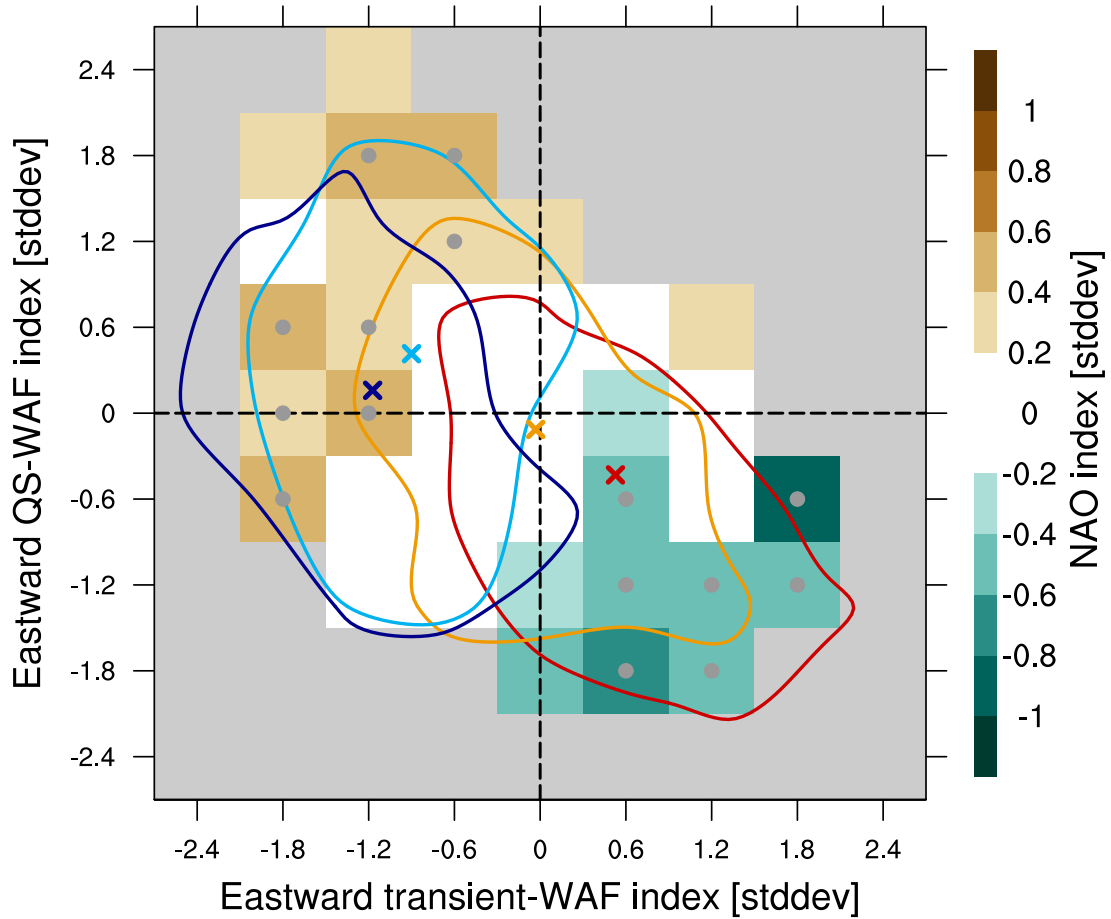


Figure 10. December to March monthly mean NAO index (color shading) as a function of the standardized eastward transient WAF (M_x) and the QS WAF (F_x) indices (definition in the main text) for the five simulations with stratospheric nudging (a total of 396 years). Grey dots in the middle of each cell indicate statistically significant values at the 95% confidence level according to a t-test with at least 10 data points. Light grey cells correspond to combinations of the WAF indices with less than 10 events. Colored contours represent the 2D-distribution of the number events for each ENSO experiment (red: strong EN, orange: moderate EN, light blue: moderate LN, dark blue: strong LN), where only the 10 events contour is shown for clarity, and where crosses indicate the mean values of the WAF indices for each of the ENSO forcing simulations.

Table 1. Frequency of extreme strong and weak eastward transient (M_x -index) and quasi-stationary (F_x -index) monthly WAF events. Asterisks * and double asterisks ** indicate that the mean value of the index distribution is statistically different from the climatological simulation at the 90% and 95% confidence level, respectively.

Nudged stratosphere	Strong EN	Moderate EN	Climatology	Moderate LN	Strong LN
M_x -index > 1.5 stddev.	13.3%**	2.8%	7.9%	0.3%**	0.3%**
M_x -index < -1.5 stddev.	1.0%**	2.2%	5.0%	16.8%**	28.8%**
F_x -index > 1.5 stddev.	5.1%**	6.3%**	6.3%	15.5%**	8.9%*
F_x -index < -1.5 stddev.	12.3%**	5.4%**	3.8%	0.3%**	2.3%*